Optimisation of Process Parameters in ECM by using Rotary U Shaped Tool

Rahul Ganjir
(209ME2198)

Department of Mechanical Engineering
National Institute of Technology Rourkela
Rourkela-769 008, Orissa, India
May 2010

Optimisation of Process Parameters in ECM by using Rotary U Shaped Tool

Thesis submitted in partial fulfilment
of the requirements for the degree of

Master of Technology

in

Mechanical Engineering

by

Rahul Ganjir
(209ME2198)

under the supervision of

Prof. C. K. Biswas

Department of Mechanical Engineering
National Institute of Technology Rourkela
Rourkela-769 008, Orissa, India
May 2010

Department of Mechanical Engineering
National Institute of Technology Rourkela
Rourkela-769 008, Orissa, India

Certificate

This is to certify that thesis entitled, **"Optimisation of Process Parameters in ECM by using Rotary U Shaped Tool"** submitted by **Mr. Rahul Ganjir** in partial fulfillment of the requirements for the award of Master of Technology in Mechanical Engineering with "Production Engineering" Specialization during session 2009-2011 in the Department of Mechanical Engineering National Institute of Technology, Rourkela. It is an authentic work carried out by him under my supervision and guidance. To the best of my knowledge, the matter embodied in this thesis has not been submitted to any other University/Institute for award of any Degree or Diploma.

Dr. C. K. Biswas
Associate Professor
Department of Mechanical Engineering
National institute of technology, Rourkela

Place
Date

Acknowledgement

I express my deep sense of gratitude and indebtedness to my thesis supervisor Dr. C. K. Biswas, Associate Professor, Department of Mechanical Engineering for providing precious guidance, inspiring discussions and constant supervision throughout the course of this work. His timely help, constructive criticism, and conscientious efforts made it possible to present the work contained in this thesis.

I express my sincere thanks to Mr. Shailesh Kumar Dewangan, Research Scholar and Mr. A. Prabhakar. I am grateful to Prof. R. K. Sahoo, Head of the Department of Mechanical Engineering for providing me the necessary facilities in the department. I express my sincere gratitude to Prof. S. S. Mahapatra, coordinator of Mechanical Engineering course for his timely help during the course of work. I am also thankful to all the staff members of the department of Mechanical Engineering and to all my well-wishers for their inspiration and help. And also to thanks my classmate's Mr. Kamal Kumar Kanujia during the help my project.

I feel pleased and privileged to fulfill my parent's ambition and I am greatly indebted to them for bearing the inconvenience during my M Tech. course.

Rahul Ganjir

Abstract

Electrochemical machining (ECM) has established itself as one of the major alternatives to conventional methods for machining hard materials and complex contours without the residual stresses and tool wear. ECM has extensive application in automotive, petroleum, aerospace, textile, medical and electronic industries. Studies on Material Removal Rate (MRR) are of utmost importance in ECM, since it is one of the determining factors in the process decisions. So the aim of present work is to investigate the MRR, overcut diameter and overcut depth of AISI P20 work piece by using a rotating copper U-tube tool. Four parameters were chosen as process variables: Feed rate, Voltage, Electrolyte concentration and Tool diameter.

The results of experiment show the material removal increase with increasing the feed, voltage and electrolyte concentration but decreases with increasing the tool diameter, and for both overcut diameter and overcut depth they increases with increasing feed ,voltage and electrode diameter but decreases with increasing electrolyte concentration. Grey relation grade (GRD) was also applied to identify the optimal parameter setting in the experiment.

Keywords: Electrochemical Machining (ECM), Taguchi Method, Metal Removal Rate (MRR), Overcut (OC), Grey Relation Analysis (GRA).

Contents

List of Figures

List of Tables

Chapter 1

Introduction

Electrochemical machining (ECM) was developed to machine difficult-to cut materials, and it is an anodic dissolution process based on the phenomenon of electrolysis, whose laws were established by Michael Faraday [1]. In ECM, electrolytes serve as conductors of electricity. The rate of machining does not depend on the hardness of the metal. ECM offers a number of advantages over other machining methods and also has several disadvantages:

Advantages: there is no tool wear; machining is done at low voltage compared to other processes with high metal removal rate; no burr formation; hard conductive materials can be machined into complicated profiles; work-piece structure suffer no thermal damages; suitable for mass production work and low labour requirements.

Disadvantages: a huge amount of energy is consumed that is approximately 100 times that required for the turning or drilling of steel; safety issues on removing and disposing of the explosive hydrogen gas generated during machining; not suited for nonconductive materials and difficulty in handling and containing the electrolyte [2].

Applications: ECM is widely used in manufacturing for making moulds and dies; also used for making complicated shape of turbine blades and it is now routinely used for the machining of aerospace components, critical deburring, Fuel injection system components, ordnance components etc.

As shown in Figure 1.1, the shaped tool (cathode) is connected to the negative polarity and the work-piece (anode) is connected to the positive polarity. The electrolyte flow through the small inter-electrode gap, thus flushing away sludge and heat generated during machining process.

1.1. Fundamental Principles

During ECM, there will be reactions occurring at the electrodes i.e. at the anode or work-piece and at the cathode or the tool along with within the electrolyte. Ion and electrons crossing phase boundaries (the interface between two or more separate phases, such as liquid-solid) would result in electron transfer reaction carried out at both anode and cathode.

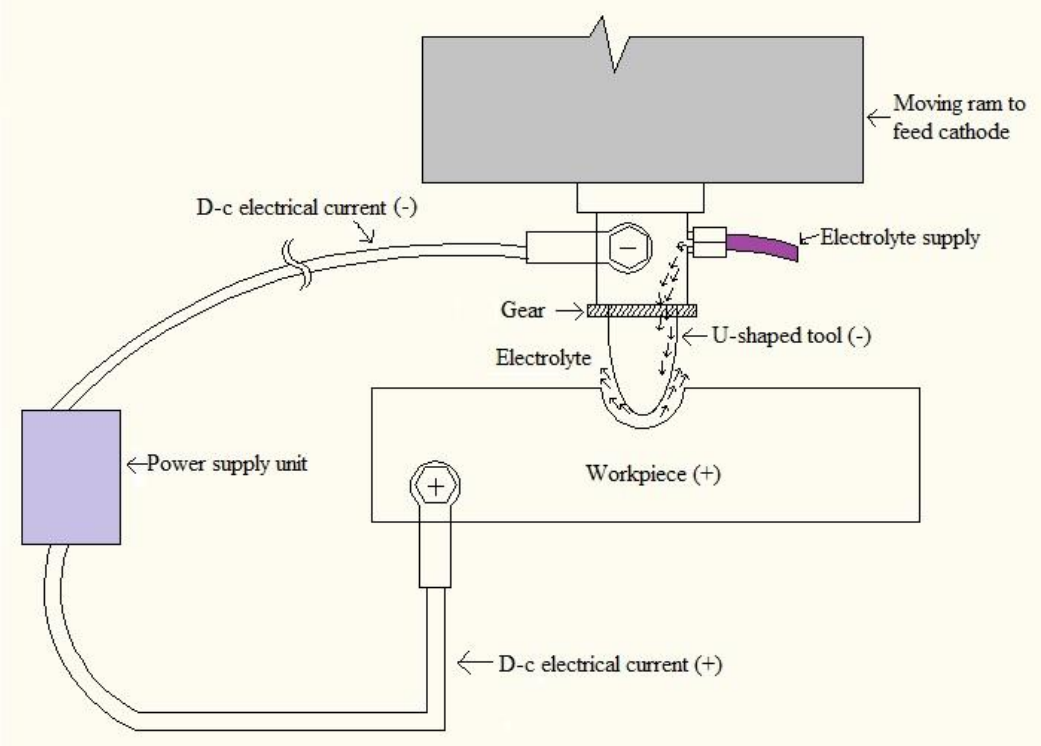

Figure 1.1: Principle of Electrochemical Machining

Meanwhile, the potential difference is fundamental in understanding the energy distribution during the electrochemical machining process. Figure 1.2 shows the broad concepts and basic potential calculation methods. Nernst equation is used to calculate the electrode reversible potential. Tafel equation, diffusion layer, and ohm's law can assist in estimating activation overpotential, concentration overpotential, and resistance overpotential, which are known as the three main overpotentials in electrochemical reactions.

1.2. ECM Machine Parameters:

1.2.1. Servo System:

The servo system controls the tool motion relative to the work piece to follow the desired path. It also controls the gap width within such a range that the discharge process can continue. If tool electrode moves too fast and touches the work piece, short circuit occurs. Short circuit contributes little to material removal because the voltage drop between electrodes is small and the current is limited by the generator. If tool electrode moves too slowly, the gap becomes too wide and electrical discharge never occurs. Another function of servo system is to retract the tool electrode when deterioration of gap condition is

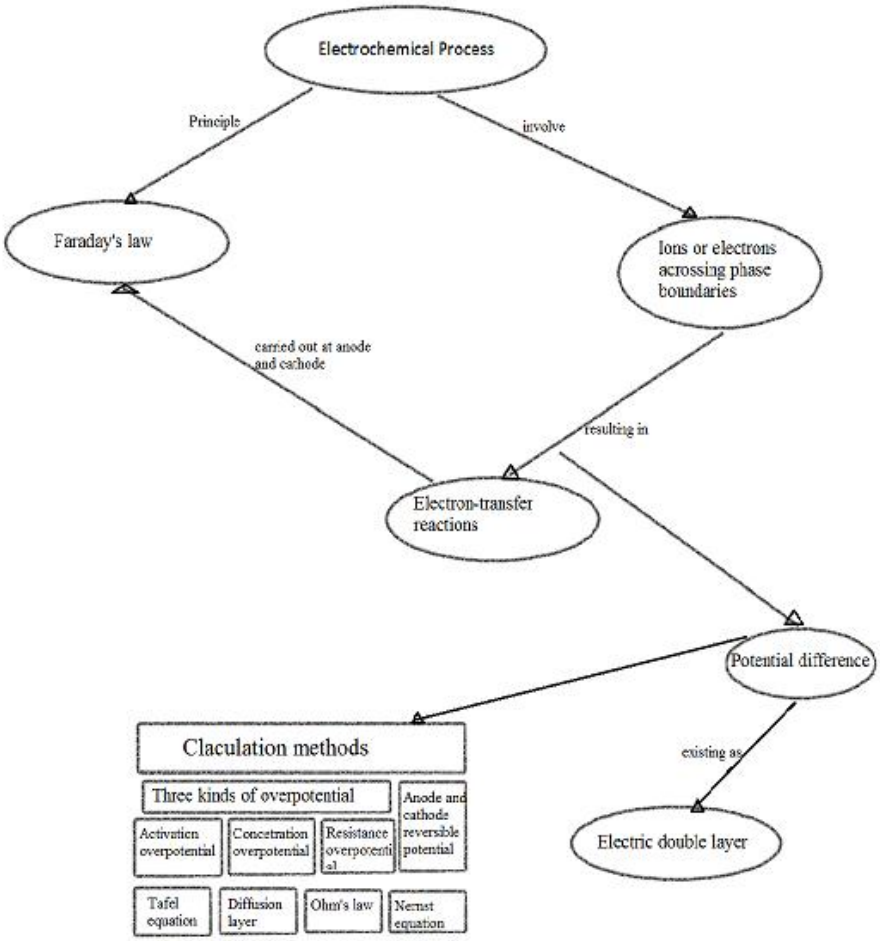

Figure 1.2 Overall concepts and calculation methods for potentials

Detected. The width cannot be measured during machining; other measurable variables are required for servo control.

1.2.2. Electrolyte:

The electrolyte is essential for the electrolytic process to work. The electrolyte has three main functions in ECM. These three functions are:

1. It carries the current between the tool and the work-piece.

2. It removes the products of machining from the cutting region.

3. It dissipates heat produced in the operation.

Electrolytes must have high electrical conductivity, low toxicity and low corrosiveness. The electrolyte is pumped at about 14 kg/cm^2 and at speed of at least 30 m/s.

1.2.3. Tool Feed Rate:

In ECM process gap about 0.01 to 0.07 mm is maintained between tool and work piece. For smaller gap, the electrical resistance between the tool and work is least and the current is maximum and accordingly maximum metal is removed. The tool is feed in to the work depending upon the how fast the metal is to be removed. The movement of the tool slide is controlled by a hydraulic cylinder giving some range of feed rate.

1.2.4. Material Removal Rate:

It is a function of feed rate which dictates the current passed between the work and the tool. As the tool advances towards work, gap decreases and current increases which increases more metal at a rate corresponding to tool advance. A stable spacing between tool and work is thus established. It may be noted that high feed rate not only is productive but also produces best quality of surface finish. However feed rate is limited by removal of hydrogen gas and products of machining. Metal removal rate is lower with low voltage, low electrolyte concentration and low temperature.

The primary advantages of the metal removal rate process are that they do not cause certain undesirable surface effects which occurred in conventional machines. The main advantages are that they are stress free machining, burr free surfaces, reduced tool wear and elimination of thermal damage to the work-piece. These processes have no effect on mechanical properties such as yield strength, ultimate tensile strength, ductility, hardness etc.

1.2.5. Tool Design:

As no tool wear takes place, any good conductor is satisfactory as a tool material, but it must be designed strong enough to withstand the hydrostatic force, caused by electrolyte being forced at high speed through the gap between tool and work. The tool is made hollow for drilling holes so that electrolyte can pass along the bore in tool. Cavitation, stagnation and vortex formation in electrolyte flow must be avoided because these result a poor surface finish. It should be given such a shape that the desired shape of job is achieved for the given machining condition.

Both external and internal geometries can be machined with an electrochemical machine. Copper is often used as the electrode material. Brass, graphite, and copper-tungsten are also often used because of the ability to be easily machined, they are conductive materials, and they will not corrode.

There are two major aspects of tool design. These are:

1. Determining the tool shape so that the desired shape of the job is achieved for the given machining conditions.

2. Designing the tool for considerations other than e.g. electrolyte flow, insulation, strength and fixing arrangements.

1.2.6. Pumps:

Single or multi-stage centrifugal pumps are used on ECM equipment. A minimum flow rate 15 litres/min per 1000 A. Electrolyzing current is generally required. A pressure of 5-30 kg/cm^2 meets most of the requirements of ECM application.

1.2.7. Filtration and Storage Tank:

The filtration of electrolyte is essential to prevent small particles of grit, metal, plastics and products of machining from entering the machining gap and causing interference in the process, for these a 5 micron polypropylene pleated filter cartridge have been used with stainless steel housing arrangement . These filters get clogged and need cleaning once in 30 hrs.

1.2.8. Valves and Piping:

The piping and control valves which supply electrolyte to the ECM tooling, must not introduce foreign matter into the electrolyte. Stainless steel is the most suitable material for valves and piping. Materials such as fibre glass and reinforced plastics are used with some degree of success.

1.3. Thesis Organization

The rest of the thesis is organized as follows.

Chapter 2 consists of a literature review based on the ECM tool design, ECM surface finish and review based on the effect of electrolyte concentration on response.

Chapter 3 present the experimental setup and tool design.

Chapter 4 present the result and discussion i.e. which process parameter effect more to MRR, overcut diameter and overcut depth.

Chapter 5 makes the conclusions and offers recommendations into future research.

Chapter 2

Literature Survey

In this chapter, we broadly classify all the research paper into three different categories, i.e. paper related to tool design, related to surface finish and some paper related to type of electrolyte used.

2.1. Overview based on tool design on ECM

D. Zhu et al. [3] proposes a finite element approach to accurately determine the electrode profiles. The proposed method does not require Iterative redesign process, therefore provides excellent convergence and efficient computing. Tool design In ECM mainly deals with predicting gap distribution for a given work-piece shape. Accurate design of tool shape is decisive to machining accuracy. In this paper experiment were conducted with 150 g/l of electrolyte ($NaCl$) and the anode is low carbon steel. In ECM experiment, an average deviation of less than 4% between experimental and theoretical results has been observed.

Yuming Zhou et al. [4] suggest a new approach for the problem like limited applicability, inaccuracy, and non-convergence occurred when tool (cathode) design in electrochemical machining has been overcomes by employing a finite element method with an optimization formulation. With the flexibility of the finite element method, even cathodes with corners, edges and cusps could be designed, provided that suitable representations are employed. Overall, the approach put forth here holds great promise for practical tool design in electrochemical machining processes.

C. S. Chang et al. [5] presented the effect of thermal fluid properties in the numerical simulation of the tool shape for given work-piece shape in electrochemical machining. A bubbly two-phase, one-dimensional flow model and a one-phase, two-dimensional flow model are applied to predict the fluid field of the electrolyte, respectively. Results show that the void fraction is the most important factor in determining the electrolyte conductivity and the shape of the work-piece. The effect of the thermal-fluid properties should be considered in the inverse problem and the relative error of corresponding work-piece can be reduced to about 0.002 when proper machining condition are chosen.

S. J. Ebeid et al. [6] studied the improvement of machining accuracy in ECM by hybridizing the process by low-frequency vibrations. The study highlights the development of mathematical models for correlating the inter relationships of various machining parameters such as applied voltage, feed rate, back pressure and vibration amplitude on overcut and conicity for achieving high controlled accuracy. This work is based on response surface methodology (RSM) approach. Hybridization techniques are applied to ECM to improve its performance. The present work addresses the improvement of machining accuracy in ECM by hybridizing the process by low-frequency vibrations. The object of the tool vibrations during the ECM process is to provide a new and improved method for ECM which:

1. Destroys the passivation layer and thereby controls the ECM action;
2. Utilizes a reciprocal motion between the tool and work-piece to pump and consequently enhance the circulation of the electrolyte through the interface to permit the use of high current densities in order to improve the quality of the machined surface.

The response surface methodology used in the present work has proved its adequacy to be an effective tool for the analysis of the ECM process and the amplitude of the tool vibration is the most effective parameter affecting ECM accuracy. However, this effect diminishes after the tool amplitude reaches 80 µm.

P. S. Pa [7] studied the most effective geometry for the design electrode in electrochemical smoothing following end turning is investigated. Through simple equipment attachment, electrochemical smoothing can follow the cutting on the same machine. When adequate work-piece rotational speed associated with higher electrode rotation produces better polishing. The electrode of the partial curve with a small line diameter performs the best for the electropolishing. Electrochemical smoothing saves the need for precise turning, making the total process time less than the electrobrightening. But the electrobrightening after precise turning only requires quite a short time to make the work-piece bright. The use of ultrasonic in the electrochemical smoothing and the electrobrightening is more evident than the pulsed current, since the ultrasonic-aided process exempts off time and obtains a better polishing result.

Chunhua Sun et al. [8] proposes an approach using finite element method (FEM) to design tool in ECM. It is capable to design three dimensional freeform surface tool form the scanned data of known work-piece. In the present work, he developed a technique that is capable of

handling three-dimensional tool design based on the Laplace's equation of the practical potential field with the FEM. The proposed method can deal with the three dimensional tool design and has high computing efficiency, good accuracy and flexible boundary treatment. It combines tool design in ECM with the technology of CAD/CAM and makes ECM tool design procedure relatively inexpensive within shorter lead time.

J. A. Westley et al. [9] presented a paper to studied electrolyte flow, the problems occurring during development and to derive generic design solutions arising. In addition, it was required to identify factors, such as insulation requirements and machined face considerations that could relate to other ECM components. The main considerations for ECM tooling are the flow of the electrolyte solution. If the electrolyte is restricted as it exits from the flow slot, there is a very high risk of a spark occurring between the electrode and the workface. The results shows some point to be consider when ECM tool design these are the path of electrolyte flow should be as unrestricted as possible, electrolyte exit slots should be of a continuous from without V-slots or enlargements and interior of the electrolyte exit slot should be as flat as possible.

Amalnik and McGeough [10] has reported that an intelligent knowledge-based system (IKBS) for evaluating electrochemical machining, in a concurrent engineering (CE) environment and based on object oriented techniques, is introduced. The design specification is acquired through a feature-based approach. Ten different classes of design features are interactively obtained. The attributes of 72 work piece material types, eight tool-electrode metals, two electrolyte solutions, and seven different sizes and types of electrochemical machines are stored in a database. For each design feature, information needed in manufacturing, such as the machining cycle time and cost, penetration rate, efficiency and effectiveness, costs for electricity consumed, machine installation and depreciation are estimated. Finally, for the same design specification, machining times are compared and ordered, for alternative unconventional processes of electrochemical, electro-discharge and electrochemical arc machining.

2.2. Overview based on surface finish on ECM process

K. P. Rajurkar and M. S. Hewidy [11] presented a paper to examine two aspects of ECM performance. The reduction in the experimentally measured values of the final gap with the increase in work specimen grain size is used to develop a correction factor. The prediction of

the anode profile based on the correction factor and the improved *cosθ* method compares well with the anode cavity profile measured with a specially designed and built instrument. The result found that the final inter-electrode gap, the current, the machining rate, and surface roughness are influenced by the grain size. An experimentally measured set of the final gap values are used in conjunction with the improved *cosθ* method to predict the anode shape for work-pieces of different grain size. The surface profiles have been modelled and analysed by a stochastic methodology called Data Dependent Systems (DDS) for wavelength decomposition. The Green's function of the ECM surface profiles is correlated with the distribution of potential gradient or current over the work-piece surface profile.

K. P. Rajurkar et al. [12] focus on minimizing the material to be removed by predicting minimum machining allowance and improving the degree of localized dissolution. the anode dissolution should be maximum at higher current densities and almost zero at lower current densities. The results suggest the effectiveness of using proper short pulse to achieve a higher degree of localized dissolution. It is found that pulse ECM with an on-time of 1-3ms and a duty factor of 50% provides optimum estimates for desired dimensional accuracy. The passivating electrolyte such as $NaNO_3$ exhibits better machinability characteristics. Approximately 35% reduction in material to be removed is estimated by the use of PECM with $NaNO_3$ electrolyte.

M. S. Hewidy [13] developed new technique to utilize a simultaneously moving and rotating electrode to remove a specific amount of material from pre-machined holes and rods of hardened steel specimens. One of the electrodes was provided with two simultaneous movements, traverse speed and rotational speed. Experimental results revealed that this technique could lead to the removal of a surface layer thickness up to 200µ, which consequently classified this method as a super-finishing process, shows the machining cell that has been used for hole and rod finishing. The cell has been adapted to work on a radial drilling machine to get the advantages of the controlled feed rate and the rotational motion of the tool. The electrolyte was sodium chloride (200 g/l), and has been fed into the cell through a centrifugal pump drawing from a plastic tank ($1m^3$). In the present work, the possibility of increasing feed rates has been achieved which could lead to the removal of wall thickness up to 0.02 mm. This enhances the controllability of the ECM process. Theoretical model and computer calculations facilitate the prediction of metal removal thickness through different combinations of ECM parameters.

I. Strode and M. B. Bassett [14] investigated the effect of Electrochemical machining on the surface integrity of cast and wrought steels. It is shown that the resulting surface structure and surface finish are strongly dependent on the current density used during machining, it's also indicate that the surface damage resulting from electrochemical machining is less than that obtained after electro discharge machining. The result shows some points i.e. all pre-existing surface stresses are removed during ECM, resulting in a near-stress-free surface, the reduction in fatigue strength which occurs after ECM at an adequate current density is mainly due to the removal of compressive stresses and the fatigue strength of electrochemically machined surfaces may be substantially increased by light shot peening.

Ming-Chang Jeng et al. [15] studied the effects of carbon content, microstructure and working pressure on the metal removal rate and current efficiency in electrochemical machining of carbon steels. In this paper four different carbon contents and various heat-treatment procedures (quenching, tempering and annealing) were performed. The result shows following points:

- The removal rate and current efficiency increase with carbon content,
- The quenched microstructure and the tempered microstructure have a greater removal rate and current efficiency than those of annealed microstructures,
- The work-piece machined at a working pressure of 3-4 kg/cm^2 has the greatest removal rate and current efficiency,
- The roughness of the machined surface of the annealed microstructure is greater than those of the quenched and tempered steels.

S. C. Tam and N.H. Loh [16] studied the ECM–abrasive polishing of mild steel specimens using response surface methodology (RSM). Three independent parameters: ECM voltage, electrolyte concentration and tool-holding pressure were chosen as the process variables, whilst the surface roughness of the finished specimens, R_{tm} was the response variable that had to be minimised. A minimum value of $R_{tm}$of 0.64 μm was predicted at an ECM-voltage of 5.64 V, an electrolyte concentration of 7%, and a tool-holding pressure of 0.61 bars. There are many process variables that can affect the surface finish of the ECM-abrasive polished specimens: tool spindle speed, work-piece speed, oscillation frequency, tool-holding pressure, type of abrasive, grit size, grit concentration, bond strength, electrode material, tool gap, type of electrolyte, concentration of electrolyte, flow rate of electrolyte, ECM voltage, waveform of voltage signal, work-piece material, etc. it was found that an improved surface

finish could be achieved by alteration of the process variables from the initial values chosen, guided by the predictions of the first-order model, whilst the use of a second-order central composite design afforded a "best finish" prediction that was closely confirmed by experiment.

J.J. Sun et al. [17] developed a new MREF-ECM (modulated reverse electric field electrochemical machining) polishing process for hard passive alloys surface finishing. The results obtained from the experimental study are reported in this paper. An important parameter, MREF-ECM electric field waveform is investigated to optimize the ECM polishing process for IN718. Compared to DC and MEF, MREF is a more robust polishing process for hard passive alloys, such as IN718 since the process:

- Can improve the IN718 surface finishing quality and metal removal efficiency, especially at low frequency due to the elimination of oxide film reheating by reducing oxygen concentration during the reverse period, especially using the reverse period to replace of off-time.
- Can prevent oxide film rehealing by using a cathodic peak voltage around 10 V for IN718.
- Can further reduce the surface roughness and micro-pits by using a reverse period instead of an off-time in the MREF waveform.

The MR-ECM polishing process can efficiently remove the damaged surface layer (thickness around 200±300 mm) and produce a final polished surface in a short period (20±30 s) on the surface of hard passive alloys that have been either EDM or mechanical machined.

Lee et al. [18] in this paper, the polishing mechanism of the electrochemical mechanical polishing (ECMP) technology for tooling steel SKD11 was investigated. Suitable electrochemical process parameters were evaluated. The electrochemical characteristics of a material such as active, passive and trans-passive (dissolution) can be revealed from its I–V curve. The characteristics of passive and trans-passive have great effects on the ECMP polishing mechanism. Experimental procedures included qualitative, quantitative and surface quality analyses. Qualitative analyses utilized potential state to study the I–V curves of a specific specimen in various electrolytes and electrolytic concentrations, and to find out the voltages at each electrochemical state. In quantitative analyses, the electrochemical polishing processes of the ECMP technology were conducted. From the measured and theoretical

weight losses, each process state can be verified whether or not it followed the Faraday's law. Finally, the surface roughness was measured by a surface profiler. The scanning electron microscopy (SEM) was used to observe the surface profile. The energy dispersive spectroscopy (EDS) analysis was employed to analyse the metallurgical compositions of the surface. In summary, the proposed mechanism and analyses were a good methodology in finding suitable electrochemical process parameters for ECMP technology.

Hocheng and Pa [19] has reported that the electro-chemical study, electro-polishing using a turning tool as the electrode for several die materials following turning is investigated. The proposed method uses a traveling electrode instead of the mating electrode as in conventional ECM hence the dimensional error can be controlled more effectively. Further, the method removes a certain limited amount of material, therefore the complex pre-polishing as required in the soakage electro-polishing method is eliminated. This process can be used for various turning operations including end turning, form turning, and flute and thread cutting.

Wang and Zhu [20] has reported that the variation in altitude density function (ADF) of the surface topography of mild steel during electrochemical polishing (ECP) was investigated, and the mechanism of the variation of surface roughness with polishing time was analysed**.** The results show that the variation trend of ADF with polishing time is flat-steep-flat; the variation of surface roughness results in the different distributions of surface current density, and there is a fine surface smoothness in the special period of ECP from 4 to 8 s.

2.3. Overview based on Electrolyte concentration on ECM

A. K. M. De Sllva et al. [21] studied on precision ECM process, dimensional accuracy ±2 µm, surface finish 0.01 µm Ra, has been developed using narrow Inter-electrode gaps (< 50 µm) for mass production of small (100 mm^2) component parts. The electrolyte properties, especially the concentration, play a significantly role in controlling the dimensional accuracy of precision-ECM. In the experiment the Inter-electrode gap is varied between 10 and 200 µm and the electrolyte concentration between 47 and 229 g/litre aqueous $NaNO_3$ solution. Influence of electrolyte concentration on the precision-ECM process is highlighted using empirically adjusted formulae. With low concentration electrolytes, the degree of localisation is greater, enabling higher accuracy to be realised than with high concentrations this technique has been verified using two practical examples of precision ECM.

Petr NOVAK et al. [22] studied the influence of the electrolyte composition on intergranular corrosion of various nickel alloys and of hardenable stainless steel were investigated. The nickel-base alloys remained unaffected in a solution of 15 % $NaNO_3$ + 20 %$NaClO_3$+ 65 % H_2O but suffered intergranular corrosion in solutions of $NaNO_3$ and $NaNO_3 + NaCl$. Stainless steel showed no signs of intergranular attack in any of the electrolyte solutions used. It has been found that only the alloy E1617, if machined in electrolytes containing $NaCl$ or in pure $NaNO_3$ solution, shows intergranular corrosion.

M.A. Bejar and F. Gutierrez [23] present the results of a study concerned with the determination of the current efficiency when high-speed steel is machined electrochemically with a sodium nitrate electrolyte. The tests were carried out without feed rate and at several inter-electrode voltages. The inter-electrode gap and the electrical current were measured simultaneously as a function of time. The influence of current density, concentration and temperature of the electrolyte, and flow velocity on the dissolution efficiency is determined. The experiment carried out with a high speed steel bar as a anode, a copper bar as a cathode and commercial $NaNO_3$ used as a electrolyte with three different concentration 2.5, 5 and 10% (salt weight/water weight). The results show clearly that, in the case of ECM of high-speed steel with $NaNO_3$ electrolytes, the current efficiency depends on the current density, the concentration and temperature of the electrolyte, and the flow velocity.

M.A. Bejar and F. Eterovich [24] studied the wire-electrochemical cutting of mild steel, using a passivating electrolyte of $NaNO_3$, is evaluated from the point of view of the feed rate and the side gap. The results of this evaluation permit the conclusion that by using such electrolyte the maximum feed rate can be increased and the cuts are significantly more accurate than by when using an electrolyte of $NaCl$. The experimental study was performed using as the cathode a fixed circular wire of copper, the diameter d of which was either 1.1 or 0.55 mm. The electrolyte was an aqueous solution of commercial sodium nitrate at a temperature of 30°C, at a typical concentration C of 20% w/w. The result shows the lower dissolution efficiency of $NaNO_3$ electrolytes is not reflected in the frontal material removal but in the lateral material removal. Consequently, the side gap obtained with sodium nitrate electrolytes is much narrower than the side gap obtained with sodium chloride electrolytes.

T. Haisch et al. [25] studied the Application of electrochemical machining in microsystem technologies has to take into account the role of microscopic heterogeneities of steel, e.g. of carbides. Therefore, the anodic metal dissolution of the alloyed carbon steel 100Cr6 was

investigated in $NaCl$ and $NaNO_3$ electrolytes. In flow channel experiments, high current densities up to 70 A/cm^2 and turbulent electrolyte flow velocities were applied. Insoluble carbide particles cause an apparent current efficiency >100% in $NaCl$ and >67% in $NaNO_3$. These particles are enriched at the surface in $NaCl$ solution and detected by ex situ scanning electron microscopy and energy dispersive X-ray experiments. The results show that following points:

- During the high rate anodic metal dissolution of steel 100Cr6, a solid carbon-rich surface film is built up. This film is loosely bound, if concentrated $NaCl$ solutions are used, but it is strongly attached to steel in $NaNO_3$ electrolytes.
- The surface morphology using $NaCl$ indicates a blank specimen microstructure with strong dependence on hydrodynamic conditions when using the RCE. The use of $NaNO_3$ electrolyte leads to a rough microstructure.
- The metal dissolution process in $NaCl$ may be controlled by a relatively easy diffusion of Fe^{2+} ions through a loosely bound, solid surface film directly at the specimen surface to the flowing electrolyte.

D. Zhu et al. [26] proposed an electrochemical drilling method of multiple holes in which the reverse electrolyte flow is achieved in the way of electrolyte-extraction, instead of traditional forward electrolyte flow which often causes poor electrolyte flow condition and so unstable machining process. The combining manifold is optimized to equalize electrolyte flow rate in each electrode tube. The wedge-shaped electrode tubes are adopted in order to distribute the electrolyte flow more uniformly while holes with inclination angles are processed. By the proposed technique, multiple holes with diameter of 1–2 mm and aspect ratios of 2 have been produced with good quality and efficiency. The work shows that it is feasible to machine small holes using ECD by electrolyte-extraction which presents a steady flow condition comparing to forward flow in the same flow rate. Process stability and machining accuracy of ECD on multiple holes are affected by the structure of combining manifold. In machining inclined holes, wedge shaped electrodes distribute the electrolyte flow more evenly comparing to traditional electrodes, the machining accuracy and process stability are therefore improved.

Zhao et al. [27] has reported that mechanical alloying has been carried out to synthesize a hydrogen storage alloy by milling titanium hydride and nickel. The structure and

electrochemical properties such as discharge capacity, charge-transfer, and hydrogen diffusion of the milled powders were investigated. The results of X-ray diffraction showed that an amorphous phase was formed after ball milling. The electrode potentials of the milled powders were -0.989, -0.878 and-0.941 V (vs. Hg/HgO) in the electrolyte of 6 M KOH when the milling periods were 20, 40, and 60 h, respectively. The $Ti-Ni-H$ powders milled for 60 h had a maximum discharge capacity of 102.2 mAh/g at a discharge current density of 60 mA/g. The results of the linear polarization showed that the exchange current density decreased as the hydrogen concentration within the powders decreased. The electrochemical impedance spectroscopy (EIS) demonstrated the same consequence and presented that the hydrogen diffusion decreased by decreasing the hydrogen concentration.

Minghuan Wang et al. [28] studied a machining method of the spiral internal ribs by ECM are presented. Firstly, the ECM experimental system is developed, which consists of electrolyte supply module, power supply unit, and work-piece holding device. Then, a shaped cathode was used to process the spiral-turbulated hole on the built system. In this paper, parameters affecting the machining accuracy in shape duplication and machining efficiency are analysed and discussed, especially the voltage and electrolyte concentration which have the main effect on the processed results. The material removal rate increases with the enhancement of voltages on the basis of Faraday's law. Higher efficiency could be obtained at higher voltage. So, considering the high efficiency and accuracy, the proper voltage should be selected. The results shows a shaped electrode could be prepared by ultraviolet-mask curing method and was used as the cathode in electrochemical machining of the internal helix cooling hole, With the increase of the machining voltage and electrolyte concentration, the machining accuracy in shape duplication decreases and the efficiency improves and for better machining accuracy, narrow initial gap, low voltage, and electrolyte concentration should be adopted.

2.4. Conclusion and Research Objectives

Based on the above literature review it seen that only few work has been done related to rotating tool on ECM, so this research are one step ahead for ECM. The goal of this thesis is to investigate material removal rate (MRR), overcut diameter, overcut depth in electrochemical machining of AISI P20 tool steel. The objective of this thesis can be enumerated as below:

- Conduct an experimental study to identify the factors influencing the MRR, overcut diameter and overcut depth in work-piece of electrochemical machining.
- By using Taguchi method analyse which factor effect more to response.
- According to Grey relation analysis finding which run order gives optimal setting for MRR, overcut diameter and overcut depth.

Chapter 3

Experimental setup and tool design

3.1. Experimental Objectives

To study the material removal rate (MRR), Overcut diameter and overcut depth of ECM, it is necessary to identify and understand the factors affecting the responses. The factor effecting the responses have been studied by conducting series of machining experiments using AISI P20 tool steel as work-piece. AISI P20 tool steel have several properties like it's a pre hardened high tensile tool steel strength which offers ready machinability in the hardened and tempered condition therefore doesn't require further heat treatment. This eliminates the risk, cost and waiting time of heat treatment thus avoiding the associated possibility of distortion or even cracking. Schematic diagram of ECM is shown in Figure 3.1. The effect of the different process parameters such as the voltage, feed rate, electrolyte concentration and electrode diameter has been studied and has been reported in the following chapters.

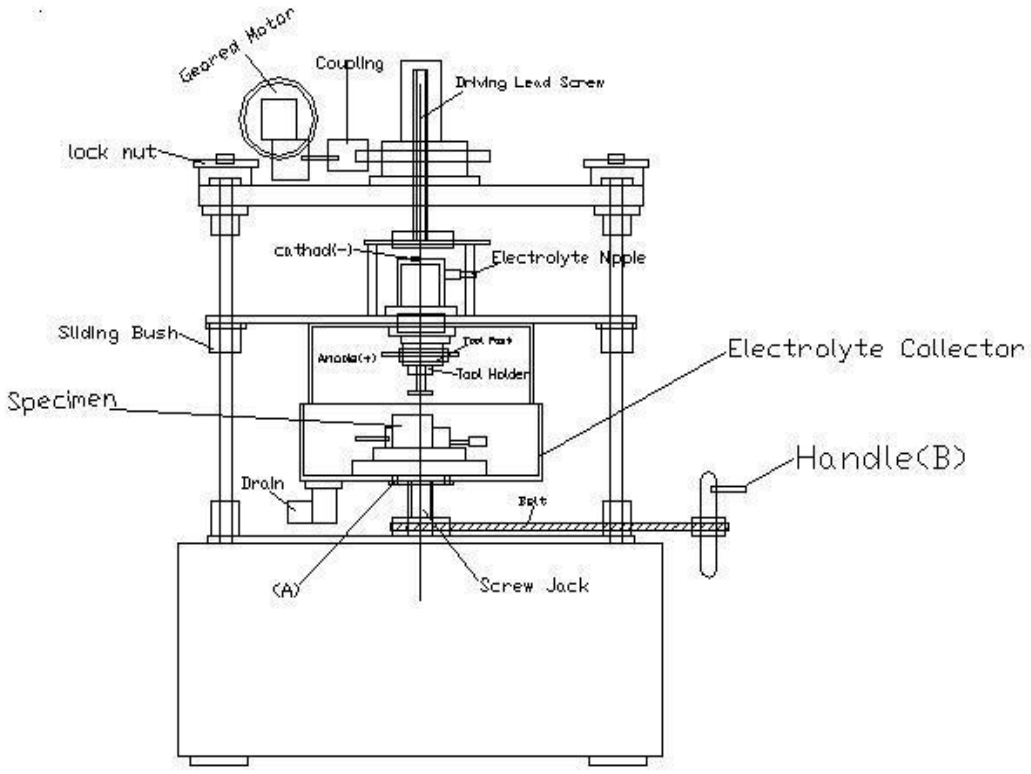

Figure 3.1: Schematic diagram of ECM

3.2. Experimental Setup

The whole experimental conducted on Electrochemical Machining set up from Metatech Industry, Pune which is having input Supply of - 415 v +/- 10%, 3 phase AC, 50 HZ. Output supply is 0-300A DC at any voltage from 0-25V and efficiency is better than 80% at partial and full load condition. The cable insulation resistance is not less than 10 Mega ohms with 500V DC. And consist of three major sub systems which are being discussed in this chapter. The set up consists of three major sub systems.

1. Machining setup
2. Control Panel
3. Electrolyte Circulation

3.2.1. Machining Setup

This electro-mechanical assembly is a sturdy structure, associated with precision machined components, servo motorized vertical up/down movement of tool, an electrolyte dispensing arrangement, illuminated machining chamber with see through window, job fixing vice, job table lifting mechanism and sturdy stand. All the exposed components, parts have undergone proper material selection and coating/plating for corrosion protection. ECM setup is shown in Figure 3.2.

Figure 3.2: ECM Setup

Technical Data

- Tool area - 30 mm^2.
- Cross head stroke - 150 mm.
- Job holder - 100 mm opening X 50 mm depth X 100 mm width.
- Tool feed motor - DC Servo type.

3.2.2. Control Panel

Through control panel we adjust the current (I), voltage (V), feed rate (F) and time (T) for duration of experiment. The power supply is a perfect integration of, high current electrical, power electronics and precision programmable microcontroller based technologies. Since the machine operates at very low voltage, there are no chances of any electrical shocks during operation. Control Panel shown in Figure 3.3.

Figure 3.3: Control Panel

Technical Data

- Electrical Out Put Rating – 0 - 300 Amps. DC at any voltage from 0 - 20 V.
- Efficiency - Better than 80% at partial & full load condition.
- Protections - Over load, Short circuit, single phasing.
- Operation Modes - Manual/Automatic.
- Timer - 0 - 99.9 min.
- Tool Feed - 0.2 to 2 mm/min.
- Z Axis Control - Forward, reverse, auto forward /reverse, through micro controller.
- Supply - 415 v +/- 10%, 3 - phase AC, 50 Hz.

3.2.3. Electrolyte Circulation

The electrolyte is pumped from a tank, lined by corrosion resistant coating with the help of corrosion resistant pump firstly it fed to filter then it's fed to the job. Spent electrolyte will return to the tank. The hydroxide sludge arising will settle at the bottom of the tank & can be easily drained out. Electrolyte supply shall be governed by flow control valve. Extra electrolyte flow is by passed to the tank. Reservoir provides separate settling and siphoning compartments. All fittings are of corrosion resistant material or of Stainless steel, as necessary.

Figure 3.4 Electrolyte tank with Filter

3.3. Tool Setup:

The purpose of the experimental investigation was to find out the Material removal rate, Overcut diameter and Overcut depth of plane work pieces made of AISI P20 tool steel.

The tools were made up of copper. It is an abridged general view of the experimental system. The experimental conditions are: the electrolyte is sodium chloride, the electrode gap between the tool and work piece is 0.1 to 0.3 mm, the work piece is 100 mm diameter and 50 mm thickness and the cathode is copper. When the experiment is carried out, the electrolyte should be at room temperature each time and after the experiment the conductivity of electrolyte must be checked. And while doing the experiment some overcuts are occurred so that overcut diameter and depth is taken with the help of Coordinate Measurement Machine (CMM).

After reviewing number of papers there is still some work that has to be done in the area of electrochemical machining with rotary tool. So in this experimental work the circular cavity is formed on the work piece by using Rotary U-shaped tubular copper electrode. So to rotate the U-shaped copper electrode, three devices are necessary as follows.

1. Gear Box.
2. Variable dc controller and
3. Rotary U- Shaped Tool electrode.

3.3.1. Gear Box

Gearboxes provide speed and torque conversion between two rotating shafts for a given gear ratio and it is a major part of this experimental setup. This gear box consists of pinion gear, face gear, double spur gear and spur gear as shown in Figure 3.5. A maximum gear ratio of 1:4 has to be maintained for speed reduction at every stage. Two gear boxes with gear ratio 1:60 were assembled in series to obtain an output speed of 0.25 rpm from a driven DC motor at 600 to 800 rpm. The speed of the motor was controlled with variable DC controller ranging from 0.5 to 3v. Figure 3.6 show the assembly of reduction gear box.

Table 3.1: Gear specifications used in the gearbox

Gear no	Name	Gear teeth (driver /driven)
1.	Pinion	10 Teeth (T)/ -
2.	Face	14 T / 36 T
3.	Double spur	14 T / 36 T
4.	Double spur	14 T / 36 T
5.	Spur	10 T / 36 T

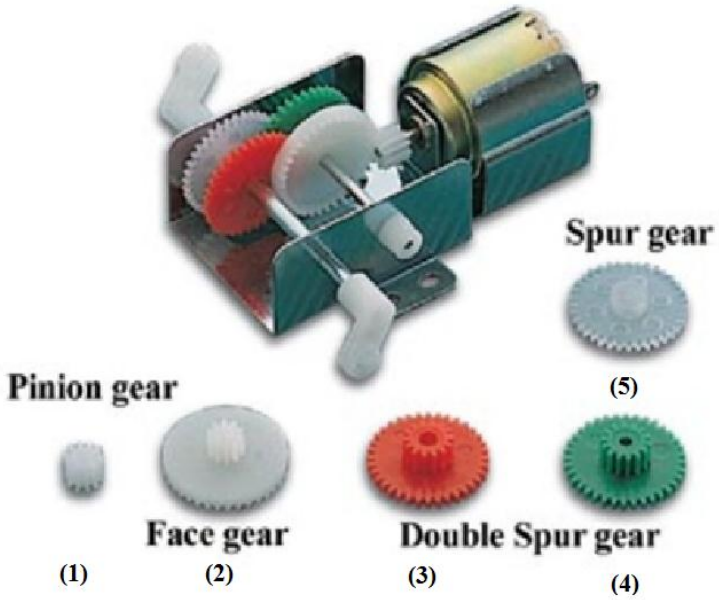

Figure 3.5: Gear Box and gears

Figure 3.6: Reduction Gear box assembly fitted in ECM machine

3.3.2. Variable DC Power Controller

Need of variable DC power supply (Figure 3.7): For Carrying out Experiments, Variable DC power supply has been used because gear box gives reduction only up to 0.25 rpm output with suitable torque. But in this experiment tool needs 0.001 to 0.1 rpm output

Figure 3.7: Variable DC controller

Circuit diagram of Variable DC Power Controller:

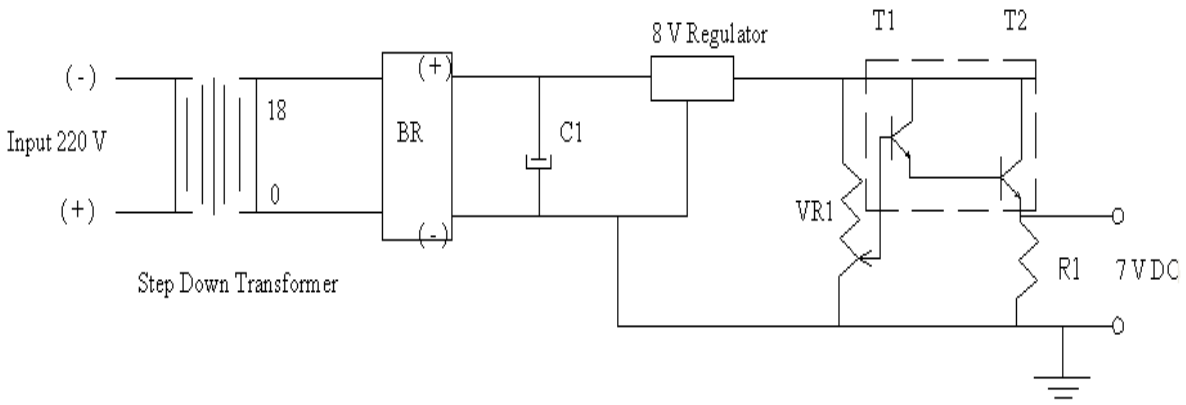

Figure 3.8: Circuit diagram of Variable DC Power supply

In Figure 3.8 shows circuit diagram of Variable DC Power Controller. It consists of step down transformer, bridge rectifier, filter rectifier, 8V regulator, Darlington pair, variable resistor and load resistor. The circuit diagram shows that input current is 220 V which goes to step down transformer where it decreases the voltage 220 V to 18 V and then it passes to Bridge rectifier where this rectifier converts AC to DC and then it goes to filter capacitor for

filtering. Filter capacitors are common in electrical and electronic work, and cover a number of applications. It filters low pass, high pass, notch, etc. and mostly used for smooth DC power supplies. After then it goes to 8V regulator where it regulates the voltage and from there it goes for Darlington Pair. A Darlington pair is used to amplify weak signals so that they can be clearly detected by another circuit. The two transistors are known as a Darlington pair. Without a Darlington pair the circuit would probably fail. And from Darlington pair it goes to variable resistor (10 turn). A variable resistor controls the amount of current flowing through part of a circuit. The amount of current can be changed by changing the setting of the resistor. The knob on a Variable DC Power Controller is a variable resistor. When the knob is turned one direction the resistance increases. This decreases or increases the current flowing and the speed can be controlled according to the requirement. After that it goes to load resistor and the output from load resistor will be given as input for the motor.

3.3.3. Rotary U-Shaped tool electrode

The U-Shaped tool electrode consists of tool holder, flexible pipes, U-shaped copper tool and 60 mm diameter plastic spur gear. In this experiment copper is taken as electrode material as cathode. U-shaped tool is designed to cut the cavity on AISI P20 tool steel in the similar profile. Two 75mm long copper pipes were taken with 4 mm and 6 mm diameters for making U-tube electrodes as shown in Figure 3.9. They were bend to the shape of U-tube. Care was taken so that circular pipe section was not distorted during bending of the copper pipes. These bend electrodes were then brazing to 50mm copper plate parallel to the axis of bending with 60 mm pipe protruding out. Ten holes were drilled on each U-shaped copper tube for the electrolyte flow freely between the work piece and tool.

Figure 3.9: U-shaped Copper Tube

A 75 mm long copper tool holder (Figure 3.10) was fabricated to support a plastic spur gear of diameter 60mm for its rotary movement which can be rotated with the help of belt drive. The tool holder has a M24 thread at the top which is inserted in ECM machine and at the bottom M12 threads support the plastic spur gear. A hole with diameter 60mm was made on the topside of tool holder which opens on both sides as shown in Figure 3.10. On both the sides, holes were made on the copper electrode and two 15mm copper pipes were brazed for fitting flexible pipes to supply electrolyte.

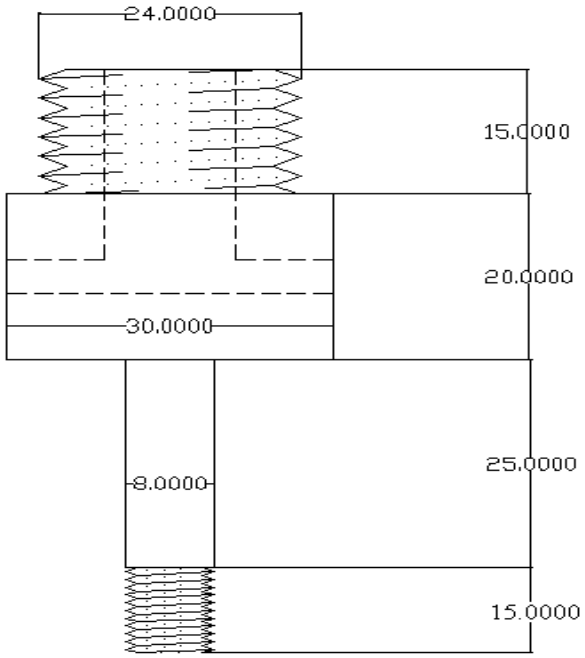

Figure 3.10: Tool Holder

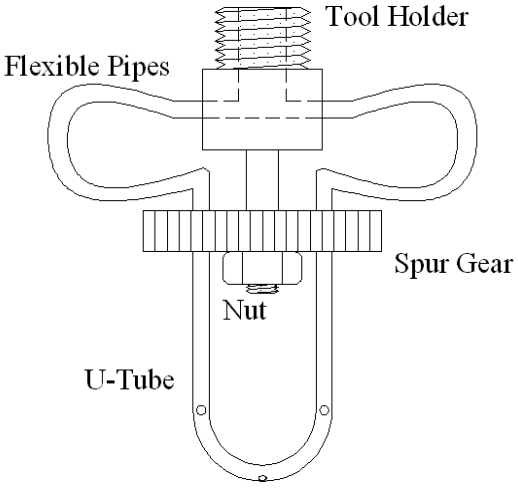

Figure 3.11: Rotary U-shaped Tool assembly

Then a plastic spur gear with diameter 60mm was taken with four equally spaced holes drilled perpendicular to each other. The U-shaped tube was inserted in two holes and was tightened with the help of brass nut bolt. After that the plastic gear was inserted into the shaft of tool holder and tightened with the nuts. Flexible pipes were affixed with copper tube which comes out of the gear as shown in Figure 3.11. A belt drive was mounted on the gear box and the plastic spur gear as shown in Figure 3.12. The U shaped tube was later electrically connected with the ECM power supply. The plastic gear and the belt serve as insulators between the ECM power supply and the electronic drive controller.

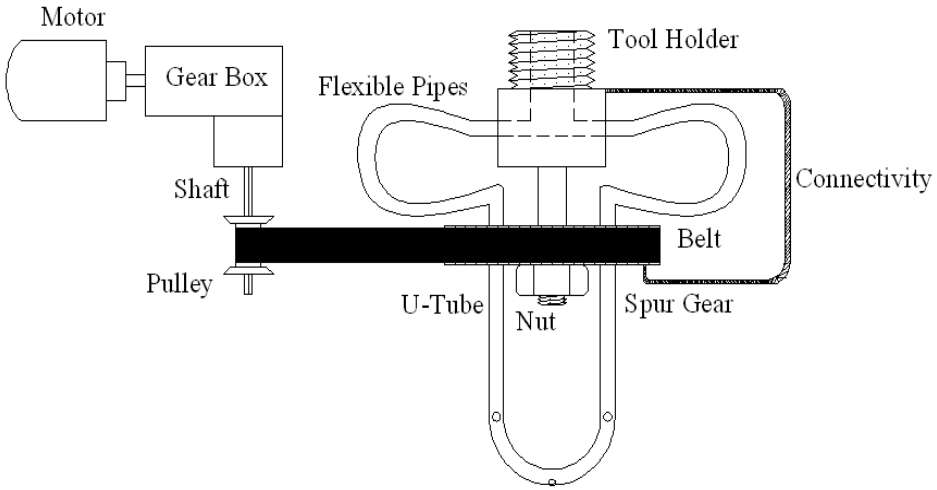

Figure 3.12: Schematic diagram of Rotary Tool

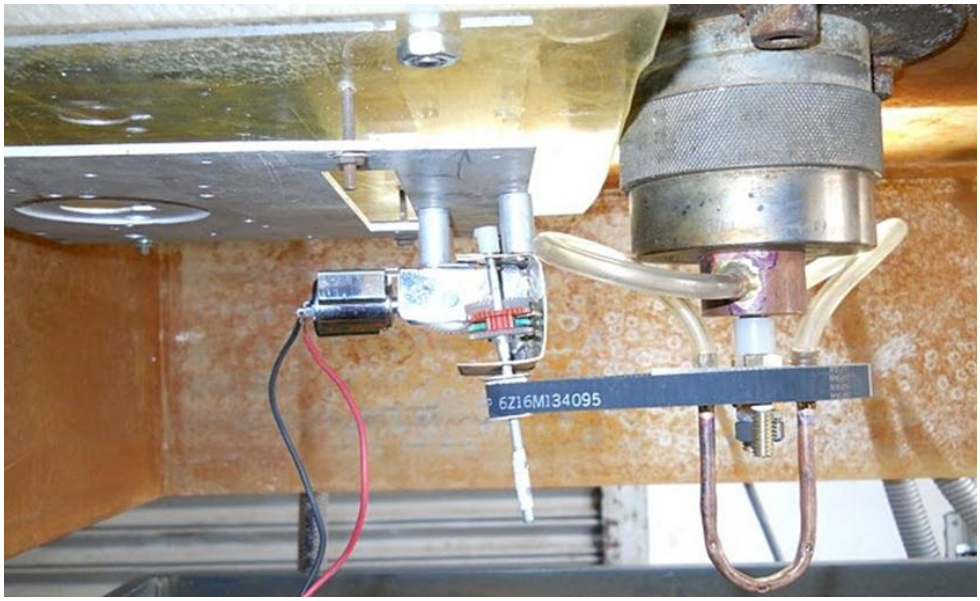

Figure 3.13: Gear arrangement with Rotary Tool

3.4 Conclusion:

A U shaped tool was designed for this experiment along with gear reduction and variable DC controller for suitable rotary feed for the experiment.

Chapter 4
Experimental Work

In this chapter experimental work is discussed which is based on Taguchi orthogonal array L16. MRR, overcut diameter and depth of the work piece were measured and Grey relational analysis is adopted to find the best parameters setting.

4.1. Specification of Work-piece material:

Experiment was conducted on AISI P20 tool steel as a work-piece. The specification of the material is given in Table 4.1 and chemical composition in Table 4.2. The mechanical and thermal properties are presented in Table 4.3. Work-piece dimension was 100 mm in diameter and 60 mm thickness. Five such pieces of AISI P20 steel were taken to conduct 16 experimental runs.

Table 4.1: Description of AISI P20 steel

Category	Steel
Class	Tool Steel
Type	General mold steel
Designations	**Germany**: DIN 1.2330 **United States**: ASTM A681, FED QQ-T-570, UNS T51620

Table 4.2: Work piece Composition

Element	C	Mn	Si	Cr	Mo	Cu	P	S
Weight %	0.28-0.40	0.60-1.00	0.20-0.80	1.40-2.00	0.30-0.55	0.25	0.03	0.03

Table 4.3: Mechanical and Thermal Properties

Parameter		Temperature(T °C)
Density (×1000 kg/m^3) at 25 ° C	7.85	25
Poisson's Ratio	0.270-0.30	25
Elastic Modulus (GPa)	190-210	25
Thermal Expansion (10^{-6}/ºC)	12.8	20-425(more)

4.2. Taguchi Experimental Design and Analysis

4.2.1. Taguchi's Philosophy

Taguchi's comprehensive system of quality engineering is one of the engineering achievements of the 20th century. His methods focus on the effective application of engineering strategies rather than advanced statistical techniques. It includes both upstream and shop-floor quality engineering. Upstream methods efficiently use small-scale experiments to reduce variability and remain cost-effective and robust design for large-scale production and market place. Shop-floor techniques provide cost-based, real time methods for monitoring and maintaining quality in production. The farther upstream a quality method is applied, the greater leverages it produces on the improvement, and the more it reduces the cost and time. Taguchi's philosophy is founded on the following three very simple and fundamental concepts:

- Quality should be designed into the product and not inspected into it.
- Quality is best achieved by minimizing the deviations from the target. The product or process should be so designed that it is immune to uncontrollable environmental variables.
- The cost of quality should be measured as a function of deviation from the standard and the losses should be measured system-wide.

Taguchi proposes an "off-line" strategy for quality improvement as an alternative to an attempt to inspect quality into a product on the production line. He observes that poor quality cannot be improved by the process of inspection, screening and salvaging. No amount of inspection can put quality back into the product. Taguchi recommends a three-stage process: system design, parameter design and tolerance design. In the present work Taguchi's design approach is used to study the effect of process parameter on the various responses of the ECM process.

4.2.2. Experimental Design Strategy

Taguchi's recommends orthogonal array (OA) for laying out of experiments. These OA's are generalised Graeco-Latin squares. To design an experiment is to select the most suitable OA and to assign the parameters and interaction of interest to the appropriate columns. The use of linear graphs and triangular table suggested by Taguchi makes the assignment of parameters simple. The array forces all experimenters to design almost identical experiments.

In the Taguchi method the results of the experiments are analysed to achieve one or more of the following objectives:

- To establish the best or the optimum condition for a product or process
- To estimate the contribution of individual parameters and interactions
- To estimate the response under the optimum condition

The optimum condition is identified by studying the main effect of each of the parameters. The main effects indicate the general trends of influence of each parameter. The analysis of variance (ANOVA) is the statistical treatment most commonly applied to the results of the experiments in determining the per cent contribution of each parameter against a stated level of confidence. Study of ANOVA table for a given analysis helps to determine which of the parameters need control.

In the present investigation the analysis of variance (ANOVA) has been performed. The effect of the selected ECM process parameters on the selected responses have been investigated through the plots of the main effects based on ANOVA. The optimum condition for each of the quality characteristics has been estimated through analysis of variance.

In the experiment, Minitab 14 software for Taguchi design was used. In this study, 2 level design (four factors) with total of 16 numbers of experiments to be conducted and hence the OA L16 was chosen. The machining parameters and their level are shown in Table 4.4.

Table 4.4 Machining parameters and there levels

Machining Parameter	Symbol	Unit	Level	
			Level 1	Level 2
Voltage	V	v	10	15
Feed Rate	F	mm/min	0.3	0.6
Electrolyte concentration	C	g/l	30	50
Electrode Diameter	D	mm	4	6
Flow rate	-	lpm	10	

4.3. Making of Brine Solution:

In the ECM process the making of brine solution plays an important role in material removal rate. Brine solution was prepared by adding common salt with

water by maintaining the conductivity of the water. In this experiment we have taken two different concentration of electrolyte i.e. 30 g/l and 50 g/l it means mixture 30 gram of salt in 1 liter of normal water and 50 gram of salt in 1 liter of normal water respectively.

4.4. Experimental Procedure:

This experiment is mainly conducted in two steps.

Step 1:

The initial weight of the work piece has to be taken for calculation of MRR. Keeping the flow rate constant at 10 l/m and the rest of the parameters are set according to Table 4.5 for each run. Work piece was kept in horizontal position, and by using the U-shaped electrode machining was started from the position "C" shown in Figure 4.1. Care has to be taken such that tip of the electrode should not touch the surface of the work-piece. The U-shaped electrode was fed up to the depth of 25mm inside the work piece. During the whole process the machining time was noted down. In this step only vertical feed motion has been taken rotation of tool has done on next step.

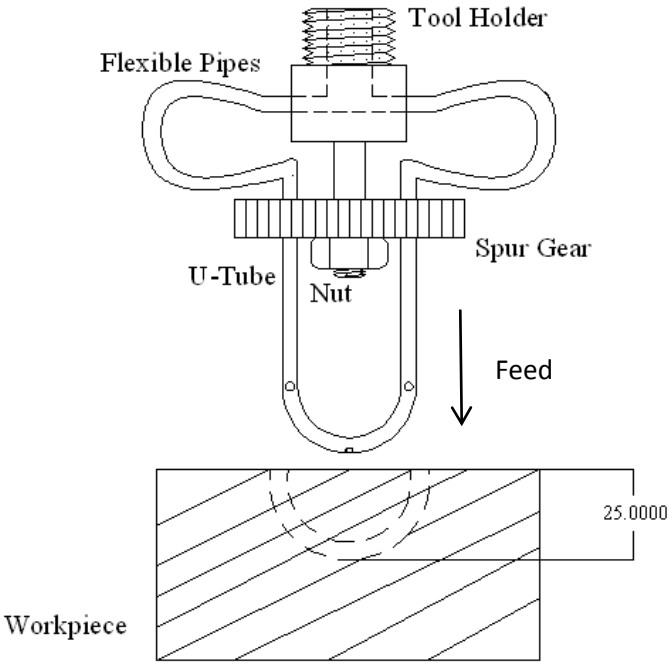

Figure 4.1: Machining step 1

Step 2:

In this step, the vertical feed of the tool was stopped and it was fed in circular direction at constant rpm. After tool rotated a half revolution, the cavity was formed

on the work-piece. The final stage after step 2 is shown In Figure 4.2. The final weight of the work-piece was noted and the machining time was being noted down.

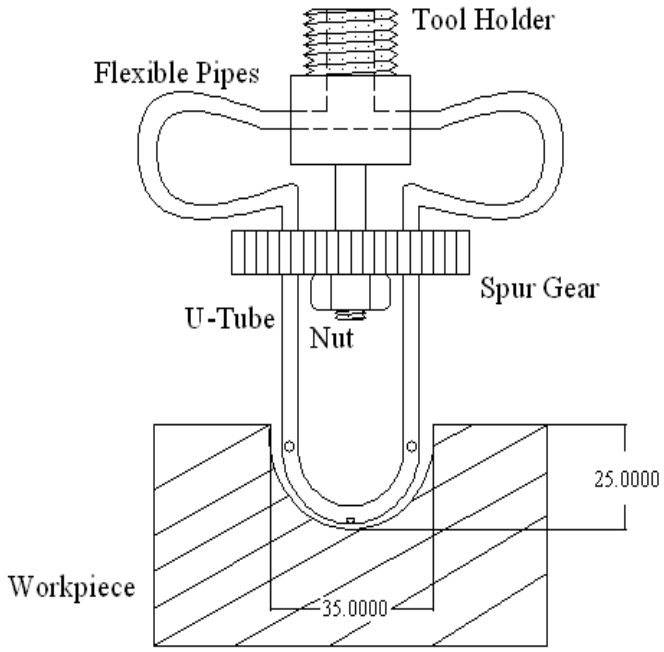

Figure 4.2: After Machining in step 2

Figure 4.3: Work-piece after machining (number inscribed represents run order)

Figure 4.3 shows the work-piece of after machining first four runs after machining. Figure 4.4 shows the work-piece of AISI P20 tool steel material after machining Run order number 5^{th}, 6^{th}, 7^{th} and 8^{th}. Figure 4.5 shows the work-piece of AISI P20 tool steel material after machining Run order number 9^{th}, 10^{th}, 11^{th} and 12^{th}. Figure 4.6 shows the work-piece of

AISI P20 tool steel material after machining Run order number 13th, 14th, 15th and 16th. The experimental observations are tabulated in Table 4.5.

Figure 4.4: Work-piece after machining 5th, 6th, 7th and 8th run

Figure 4.5: Work-piece after machining 9th, 10th, 11th and 12th run

Figure 4.6: Work-piece after machining 13th, 14th, 15th and 16th run

Table 4.5: Experimental observations using L16 orthogonal array

Run order	Voltage (V)	Feed (F) mm/min	Electrolyte concentration (C) g/l	Tool Diameter (D) mm	MRR (mm^3/min)	OC diameter (mm)	OC Depth (mm)
1	10	0.3	30	4	0.05600	4.825	6.500
2	10	0.3	30	6	0.04431	4.929	6.730
3	10	0.3	50	4	0.05830	4.812	6.287
4	10	0.3	50	6	0.05550	4.856	6.609
5	10	0.6	30	4	0.09850	5.128	6.980
6	10	0.6	30	6	0.09870	5.260	7.180
7	10	0.6	50	4	0.10800	5.089	6.830
8	10	0.6	50	6	0.09890	5.212	7.080
9	15	0.3	30	4	0.09120	4.893	6.620
10	15	0.3	30	6	0.07970	4.972	6.880
11	15	0.3	50	4	0.09110	4.853	6.474
12	15	0.3	50	6	0.08880	4.966	6.830
13	15	0.6	30	4	0.13510	5.207	7.274
14	15	0.6	30	6	0.12800	5.301	7.410
15	15	0.6	50	4	0.13640	5.208	7.140
16	15	0.6	50	6	0.12750	5.256	7.376

4.6. Sample Calculations (For run order 1):

MRR is calculated as given by the following formula:

$$\text{MRR}=\frac{\text{initial weight - final weight}}{\text{density} \times \text{total time}}$$

$$MRR = \frac{3.904 - 3.584}{0.00785 \times 755} = 0.056\ mm^3/min$$

Overcut-diameter is calculated as given by the following formula:

$$\text{OC}=\frac{\text{observed diameter - actual diameter}}{2}=\frac{\text{observed diameter-35}}{2}$$

$$OC = \frac{44.65 - 35}{2} = 4.825\ mm$$

Overcut- depth is calculated as given by the following formula:

$$\text{Overcut depth = over depth – actual depth = over depth – 25}$$

$$\text{OC}=31.5\text{-}25=6.5\ \text{mm}$$

4.7. Grey relation analysis

In the grey relation analysis, experiment data, i.e., measured responses, are first normalised in the range of 0 to 1. This process is called grey relation generation. Based on this data, grey relation coefficients are calculated to represent the correlation between the ideal (best) and the actual normalized experimental data. Overall, grey relation grade is then determined by averaging the grey relation coefficient corresponding to selected responses. The overall quality characteristics of the multi-response process depend on the calculated grey relation grade.

4.7.1. Grey relation generation

There are three different types of data normalization according to the requirement of Lower the Better (LB), Higher the Better (HB), or Nominal the Best (NB) criteria. The desired quality characteristics for MRR are HB criterion; therefore, the normalization of original sequence of these three responses is done using equation (1).

$$y_i^*(k)=\frac{y_i(k)\text{-}\min y_i(k)}{\max y_i(k)\text{-}\min y_i(k)} \quad (1)$$

Where $yi^*(k)$ is the normalised data, i.e. after grey relational generation, yi(k) is the k^{th} response of the i^{th} experiment, min yi(k) is the smallest value of yi(k) for k^{th} response, and max yi(k) is the largest value of yi(k) for the k^{th} response.

Overcut diameter and overcut depth follows the LB criterion. Accordingly, the normalization of these responses is done using equation (2).

$$yi^*(k)=\frac{\max\ yi(k)-yi(k)}{\max\ yi(k)-\min yi(k)} \tag{2}$$

4.7.2. Grey relation coefficient

The grey relation coefficient is calculated as

$$\varepsilon_i(k)=\frac{\Delta\min-\omega\Delta\max}{\Delta_{oi}(k)-\omega\Delta\max} \tag{3}$$

Where $\varepsilon_i(k)$ is the grey relation coefficient of the i^{th} experiment for the k^{th} response, $\Delta_{oi}(k)=\|y^*_0(k)-y^*_i(k)\|$, i.e. , absolute of the difference between $y^*_0(k)$ and $y^*_i(k)$, $y^*_0(k)$ is the ideal or reference sequence, $\Delta\max=\max_i \max_k\|y^*_0(k)-y^*_i(k)\|$ is the largest value of Δ_{oi} , and $\Delta min=\min_i \max_k\|y^*_0(k)-y^*_i(k)\|$ is the smallest value of Δ_{oi}, and ω ($0\leq \omega \leq 1$) is the distinguish coefficient.

4.7.3. Grey relation grade

The grey relation grade (Γ_i) is calculated by averaging the grey relational coefficients corresponding to each experiment.

$$\Gamma_i=\frac{1}{n}\sum_{=1}^{Q} i(k) \tag{4}$$

Where, Q is the total number of response and n is the number of output responses. The grey relational grade Γ_i represents the level of correlation between the reference sequence and the comparability sequence. If higher grey relation grade occurred than the corresponding parameter combination is closer to the optimal setting.

Sample calculation for Grey relation:

For run order 1

Normalised value of MRR $Y_1(MRR) = \frac{(0.056-0.04431)}{(0.1364-0.04431)} = 0.1269$

Normalised value of OC-dep $Y_1(OC\text{-}dep) = \frac{(7.41-6.5)}{(7.41-6.287)} = 0.8103$

Grey relation coefficient of MRR $\varepsilon_1(MRR) = \frac{0-0.5\times1}{(0.8731+0.5)} = 0.3642$

Grey relation coefficient of OC-dep ε_1(OC-dep) = $\frac{0-0.5\times1}{(0.1897+0.5)}$ = 0.7250

Grey relation grade of run order 1 is Γ_1 = $\frac{0.3642+0.7250}{2}$ = 0.5446

Table 4.6 Evaluated grey relational grade for responses

Run order	Normalized values		Grey relational analysis		Grey relational coefficient		Grade
	MRR	OC-dep	MRR	OC-dep	MRR	OC-dep	
1	0.1269	0.8103	0.8731	0.1897	0.3642	0.7250	0.5446
2	0.0000	0.6055	1.0000	0.3945	0.3333	0.5590	0.4462
3	0.1519	1.0000	0.8481	0.0000	0.3709	1.0000	0.6854
4	0.1215	0.7133	0.8785	0.2867	0.3627	0.6355	0.4991
5	0.5884	0.3606	0.4116	0.6394	0.5485	0.4388	0.4937
6	0.5906	0.2048	0.4094	0.7952	0.5498	0.3860	0.4679
7	0.6916	0.5165	0.3084	0.4835	0.6185	0.5084	0.5634
8	0.5928	0.2939	0.4072	0.7061	0.5511	0.4145	0.4828
9	0.5092	0.7035	0.4908	0.2965	0.5046	0.6277	0.5662
10	0.3843	0.4720	0.6157	0.5280	0.4481	0.4864	0.4673
11	0.5081	0.8335	0.4919	0.1665	0.5041	0.7502	0.6271
12	0.4831	0.5165	0.5169	0.4835	0.4917	0.5084	0.5000
13	0.9859	0.1211	0.0141	0.8789	0.9725	0.3626	0.6676
14	0.9088	0.0000	0.0912	1.000	0.8457	0.3333	0.5895
15	1.000	0.2404	0.0000	0.7596	1.0000	0.3970	**0.6985**
16	0.9034	0.0303	0.0966	0.9697	0.8380	0.3402	0.5891

Now calculate the grey relation grade for 16 number of experiment and those values have maximum in the specific run order which has closes the optimal condition. In this experiment the OC-diameter and OC-depth are co-related so, here OC-depth and MRR has been consider as responses. In Grey relational analysis of the experimental result of material removal rate and overcut depth can be simplified into the optimization of a single response that is Grey relational grade (GRG). This methodology for optimising the process parameters of ECM of P20 tool steel considering 4 input parameters and 2 output parameters. Two output responses MRR, OC-depth and there GRG for each experiment using L16 OA based on Taguchi design is shown in Table 4.6. And experimental number verse GRG plot are shown in Figure 4.7. This Figure indicates process parameter setting of Run 15 has highest grey relational grade.

Therefore, Run 15 is the optimal machining parameters setting for maximum MRR and minimum for both overcuts simultaneously among the 16 runs.

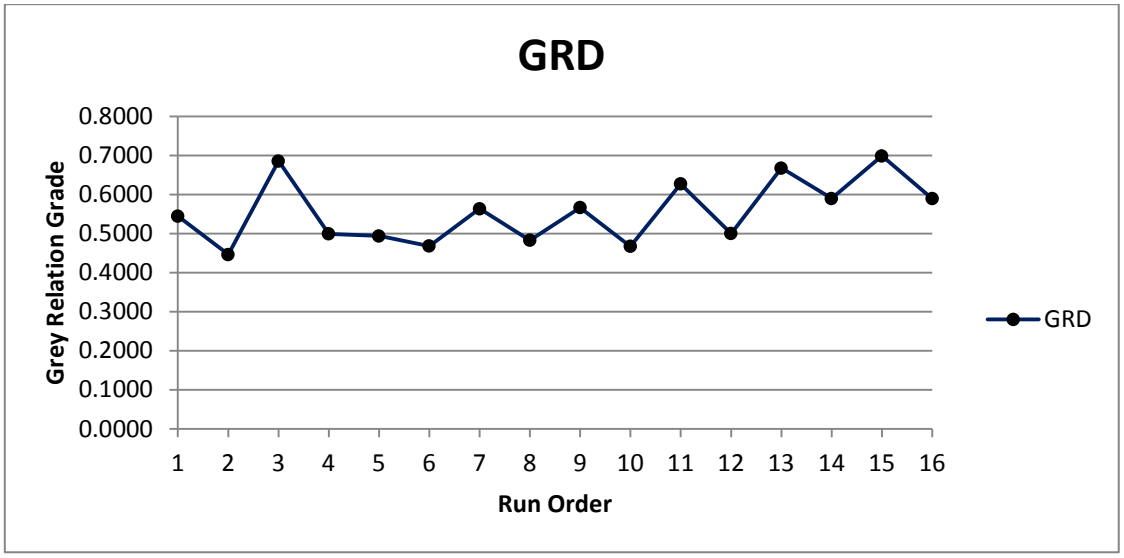

Figure 4.7: Grey Relation Grade

4.8. Conclusion

Experiments are conducted according to Taguchi method by using the machining set up and the designed Rotary U-shaped tubular electrodes. The control parameters like voltage, feed, electrolyte concentration and diameter of electrode were varied to conduct 16 different experiments. A Mould cavity can be produced by this process. The ECM process parameter setting voltage at 15v, feed 0.6 mm/min, electrolyte concentration 50 g/l and tool diameter 4 mm has highest grey relational grade. Therefore, this input parameter setting is the optimal machining parameters for maximum MRR and minimum for both overcuts simultaneously with in the experimental domain.

Chapter 5
Result and Discussion

In this chapter the effect of process parameter on responses such as MRR, Overcut diameter and Overcut depth are analysed.

5.1. Analysis of Experiment and Discussions:

5.1.1. Effect on MRR

The machinability of ECM depends on the electrical conductivity of the electrolyte, feed rate of electrode, inter electrode gap and electrolyte flow rate. The influence of various machining parameters on MRR (means) are shown in Fig. 5.1. The electrode feed rate has enormous effect on MRR and it increases with increase in feed rate. This result was expected because the material removal rate increases with feed rate because the machining time decreases. MRR also increases with voltage and electrolyte concentration; however, the effect is less than the feed rate on MRR, while by increasing the tool diameter MRR decreases and the effect of tool diameter and concentration of electrolyte has very little effect on MRR and doesn't give any conclusive evidence of any impact on MRR.

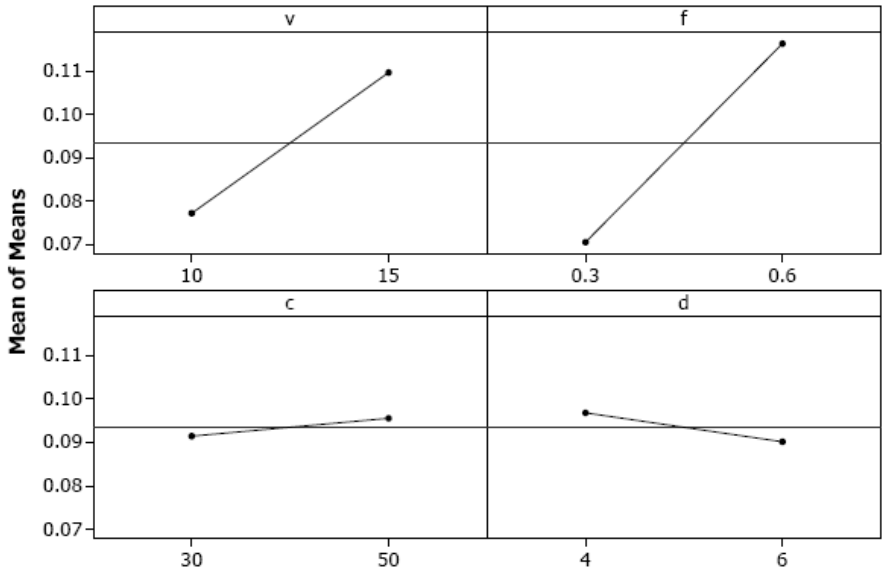

Figure 5.1: Main effect Plot for MRR

In Table 5.1, ANOVA of MRR is presented with all the terms. The columns in table represent source of variation (source), degree of freedom (DF), sequential sum of squares (Seq. SS), adjusted sum of squares (Adj. SS), adjusted mean sum of squares (Adj. MS), F-value (F), and p-value. The significant factors are Voltage, Feed and diameter of tube, whereas all interactions factors are found to be insignificant. After eliminating non-significant sources i.e. interaction of process parameter like V*F, V*D, V*D, F*C, F*D, C*D terms, the results are shown in Table 5.2.

Table 5.1: ANOVA for MRR

Source	DF	Seq. SS	Adj. SS	Adj. MS	F	P
Volt (V)	1	0.004212	0.004212	0.004212	322.46	0.000
Feed (F)	1	0.008381	0.008381	0.008381	641.68	0.000
Electrolyte Concentration(C)	1	0.000068	0.000068	0.000068	5.21	0.071
Diameter (D)	1	0.000177	0.000177	0.000177	13.54	0.014
V*F	1	0.000012	0.000012	0.000012	0.91	0.384
V*C	1	0.000011	0.000011	0.000011	0.86	0.397
V*D	1	0.000003	0.000003	0.000003	0.20	0.676
F*C	1	0.000009	0.000009	0.000009	0.69	0.445
F*D	1	0.000001	0.000001	0.000001	0.05	0.824
C*D	1	0.000003	0.000003	0.000003	0.23	0.649
Error	5	0.000065	0.000065	0.000013		
Total	15	0.012941				

Table 5.2: ANOVA for MRR after eliminating non-significant values

Source	DF	Seq. SS	Adj. SS	Adj. MS	F	P
Volt (V)	1	0.004212	0.004212	0.004212	446.66	0.000
Feed (F)	1	0.008381	0.008381	0.008381	888.83	0.000
Electrolyte Concentration (C)	1	0.000068	0.000068	0.000068	7.21	0.021
Diameter (D)	1	0.000177	0.000177	0.000177	18.75	0.001
Error	11	0.000104	0.000104	0.000009		
Total	15	0.012941				

Table 5.3: Taguchi analysis response table for MRR: larger is better

Level	Voltage (V)	Feed (F)	Concentration (g/l)	Diameter (mm)
1	0.07728	0.07061	0.09144	0.09683
2	0.10973	0.11639	0.09556	0.09018
Delta	0.03245	0.04577	0.00412	0.00665
Rank	2	1	4	3

In Table 5.3, the main effects of voltage, feed, electrolyte concentration and diameter of electrode are 0.03245, 0.04577, 0.00412 and 0.00665 respectively, on MRR in mm^3/min, in order of significance. In which there feed rate is important factor and then voltage then electrode diameter and then electrolyte concentration. These results are in good agreement with the observations of many researchers.

The coefficients of model mean of means for MRR are shown in Table 5.4. The parameter R^2 describes the amount of variation observed in MRR is explained by the input factors. R^2 = 99.2 % indicate that the model is able to predict the response with high accuracy. Adjusted R^2 is a modified R^2 that has been adjusted for the number of terms in the model. If unnecessary terms are included in the model, R^2 can be artificially high, but adjusted R^2 (=98.9 %.) may get smaller. The standard deviation of errors in the modelling, S= 0.003071. Comparing the p-value to a commonly used α-level = 0.05, it is found that if the p-value is less than or equal to α, it can be concluded that the effect is significant, otherwise it is not significant.

Table 5.4: Estimated Model Coefficients for Means of MRR

Term	Coefficient	SE Co-eff.	T	P
Constant	0.093501	0.000768	121.797	0.000
V 10	-0.016224	0.000768	-21.134	0.000
F 0.3	-0.022887	0.000768	-29.813	0.000
C 30	-0.002062	0.000768	-2.686	0.021
D 4	0.003324	0.000768	4.330	0.001
S = 0.003071		R-Sq. = 99.2%		R-Sq.(adj.) = 98.9%

The residues are calculated by the difference between the model value of MRR and the observed value of MRR. The residual plot of MRR is shown in Fig. 5.2. This layout is

useful to determine whether the model meets the assumptions of the analysis. The residual plots in the graph and the interpretation of each residual plot indicate below:

a. Normal probability plot indicates the data are normally distributed and the variables are influencing the response. Outliers don't exist in the data, because standardized residues are between -2 and 2.
b. Residuals versus fitted values indicate the variance is constant and a nonlinear relationship exists as well as no outliers exist in the data.
c. Histogram proves the data are not normally distributed it may be due to the fact that the number of points are very less.
d. Residuals versus order of the data indicate that there are systematic effects in the data due to time or data collection order.

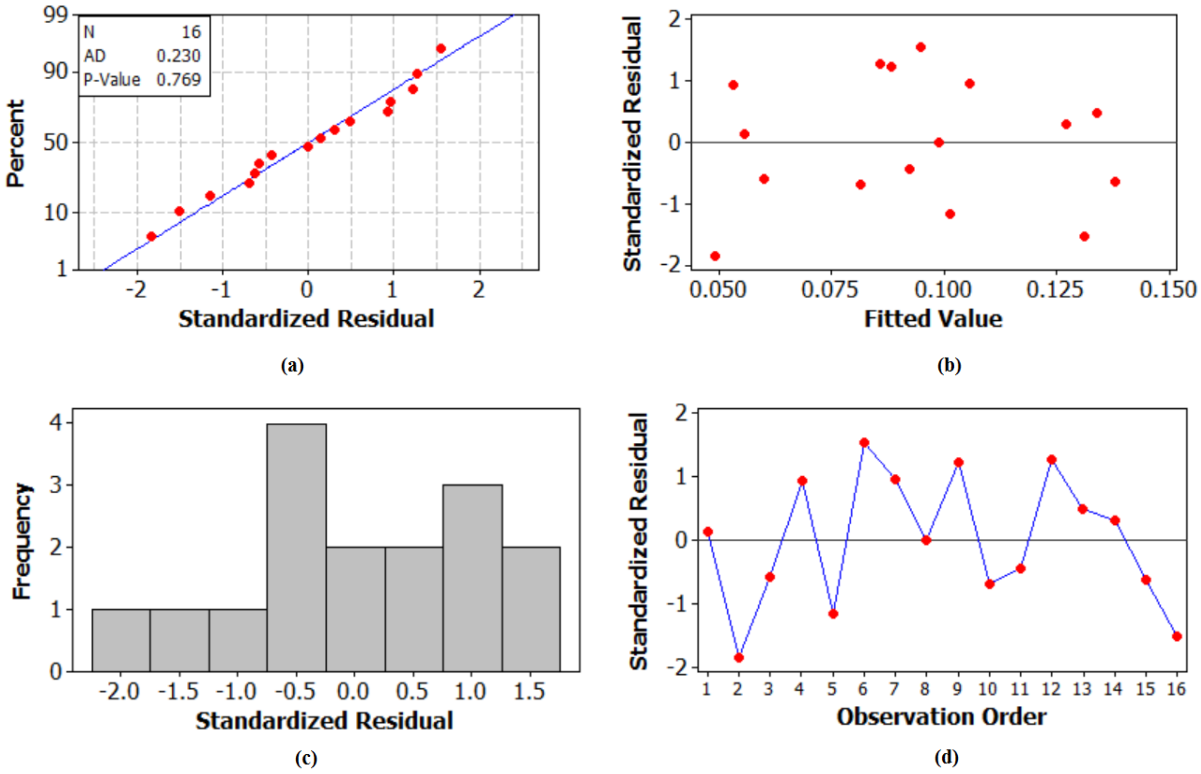

Figure 5.2: Residual Plots for MRR (a) Normal probability plot (b) Residual vs. Fitted plot (c) Histogram of Residuals (d) Residuals vs. Order of data plot

5.1.2. Effect on overcut-diameter

The influence of various machining parameters on overcut-diameter (means) are shown in Figure 5.3. The electrode feed rate has enormous effect on width over cut and it increases with increase in feed rate. Overcut-diameter also increases with larger diameter of

electrode and when increasing the voltage. While overcut diameter decreases with increasing in electrolyte concentration.

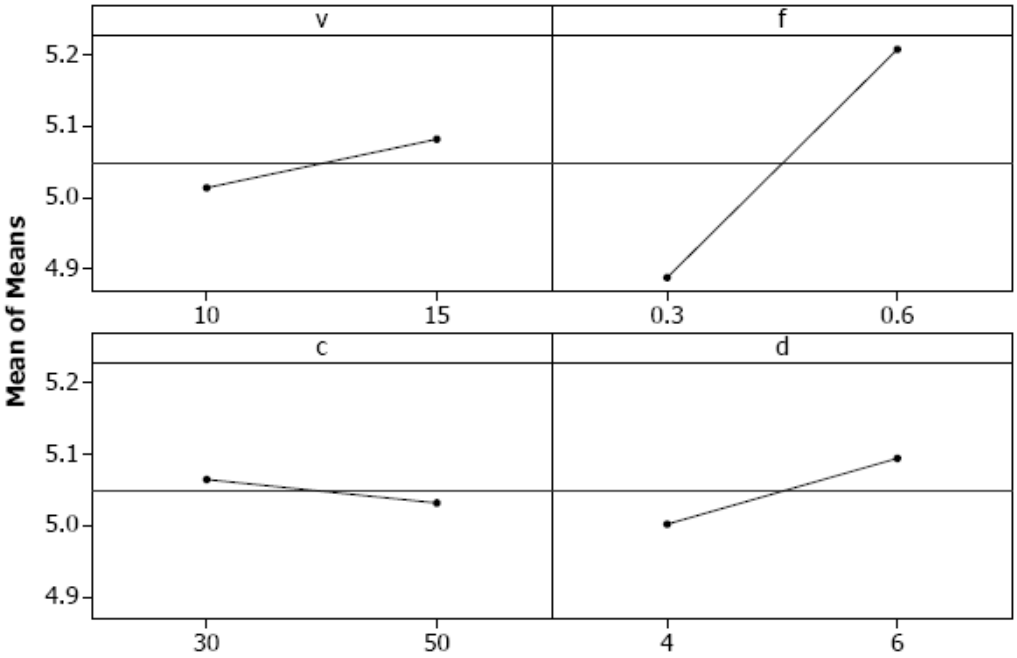

Figure 5.3: Main effect Plot for OC-diameter

Table 5.5: ANOVA for OC-diameter

Source	DF	Seq. SS	Adj. SS	Adj. MS	F	P
Volt (V)	1	0.018564	0.018564	0.018564	32.35	0.002
Feed (F)	1	0.408002	0.408002	0.408002	710.97	0.000
Electrolyte Concentration(C)	1	0.004323	0.004323	0.004323	7.53	0.041
Diameter (D)	1	0.033948	0.033948	0.033948	59.16	0.001
V*F	1	0.000028	0.000028	0.000028	0.05	0.835
V*C	1	0.000431	0.000431	0.000431	0.75	0.426
V*D	1	0.000298	0.000298	0.000298	0.52	0.504
F*C	1	0.000000	0.000000	0.000000	0.00	0.992
F*D	1	0.000203	0.000203	0.000203	0.35	0.578
C*D	1	0.000410	0.000410	0.000410	0.71	0.437
Error	5	0.002869	0.002869	0.000574		
Total	15	0.469075				

In Table 5.5, ANOVA of OC-diameter is presented with all the terms. The significant factors are Voltage, Feed, electrolyte concentration and diameter of tube, whereas all interactions factors are found to be insignificant. After eliminating non-significant sources i.e. interaction of process parameter like V*F, V*D, V*D, F*C, F*D, C*D terms, the results are shown in Table 5.6.

Table 5.6: ANOVA for OC-diameter after eliminating non-significant values

Source	DF	Seq. SS	Adj. SS	Adj. MS	F	P
Volt (V)	1	0.018564	0.018564	0.018564	48.18	0.000
Feed (F)	1	0.408002	0.408002	0.408002	1058.95	0.000
Electrolyte Concentration(C)	1	0.004323	0.004323	0.004323	11.22	0.006
Diameter (D)	1	0.033948	0.033948	0.033948	88.11	0.000
Error	11	0.004238	0.004238	0.000385		
Total	15	0.469075				

In Table 5.7 the main effects of voltage, feed, electrolyte concentration and diameter of electrode are 0.068, 0.319, 0.033 and 0.092 respectively, on overcut-diameter in mm, in order of significance. In which there feed rate is important factor and then electrode diameter then voltage and lastly is electrolyte concentration.

Table 5.7: Taguchi analysis response table for OC-diameter

Level	Voltage (V)	Feed (F)	Concentration (g/l)	Diameter (mm)
1	5.014	4.888	5.064	5.002
2	5.082	5.208	5.032	5.094
Delta	0.068	0.319	0.033	0.092
Rank	3	1	4	2

The coefficients of model mean of means for over cut shown in Table 5.8 and parameter result are standard deviation of error S=0.01963, amount of variation R^2 = 99.1% and R^2 (adj.) = 98.8%. And comparing the P value is less than or equal to 0.05 it can be concluded that the effect is significant, otherwise not significant.

Table 5.8: Estimated Model Coefficients for Means of OC-diameter

Term	Co-eff.	SE Co-eff.	T	P
Constant	5.04794	0.004907	1028.680	0.000
V 10	-0.03406	0.004907	-6.941	0.000
F 0.3	-0.15969	0.004907	-32.541	0.000
C 30	0.01644	0.004907	3.350	0.006
D 4	-0.04606	0.004907	-9.387	0.000
S = 0.01963		R-Sq. = 99.1%		R-Sq.(adj.) = 98.8%

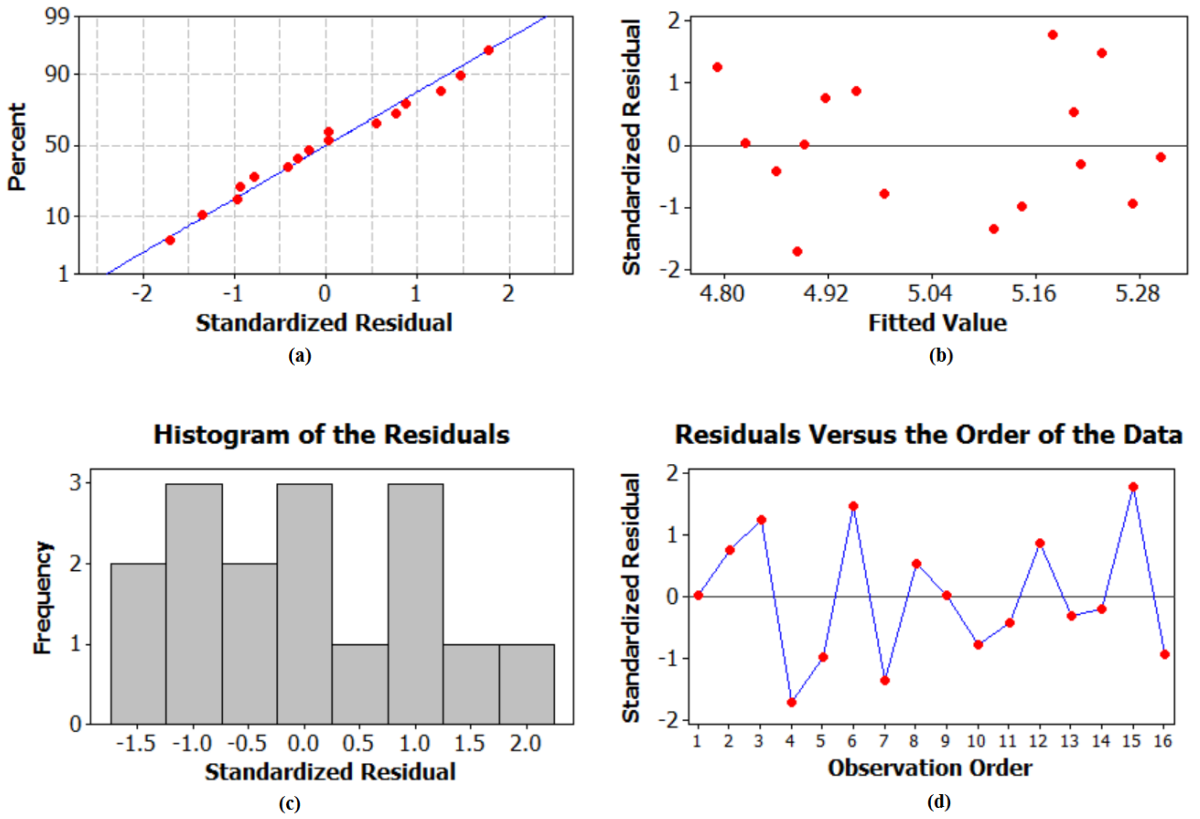

Figure 5.4: Residual Plots for OC-diameter. (a) Normal probability plot (b) Residual vs. Fitted plot (c) Histogram of Residuals (d) Residuals vs. Order of data plot

The residual plot for over cut is shown in Figure 5.4. This residual plot in the graph for normal probability plot indicates the data are normally distributed and variables are influencing the response. And the Residuals versus fitted value indicate the variation is constant. And the Histogram proved the data are not normally distributed it may be due to the fact that the number of points are very less. And Residual versus order of the data indicates that there are systematic effects in the data due to data collection order.

5.1.3. Effect on overcut- depth

The influence of various machining parameters on overcut-depth (means) are shown in Figure 5.5. The electrode feed rate has enormous effect on overcut-depth and it gradually increases with increase in feed rate also overcut-depth increases with increase of voltage and electrode diameter. While as in case of electrolyte concentration no change in overcut-depth is observed.

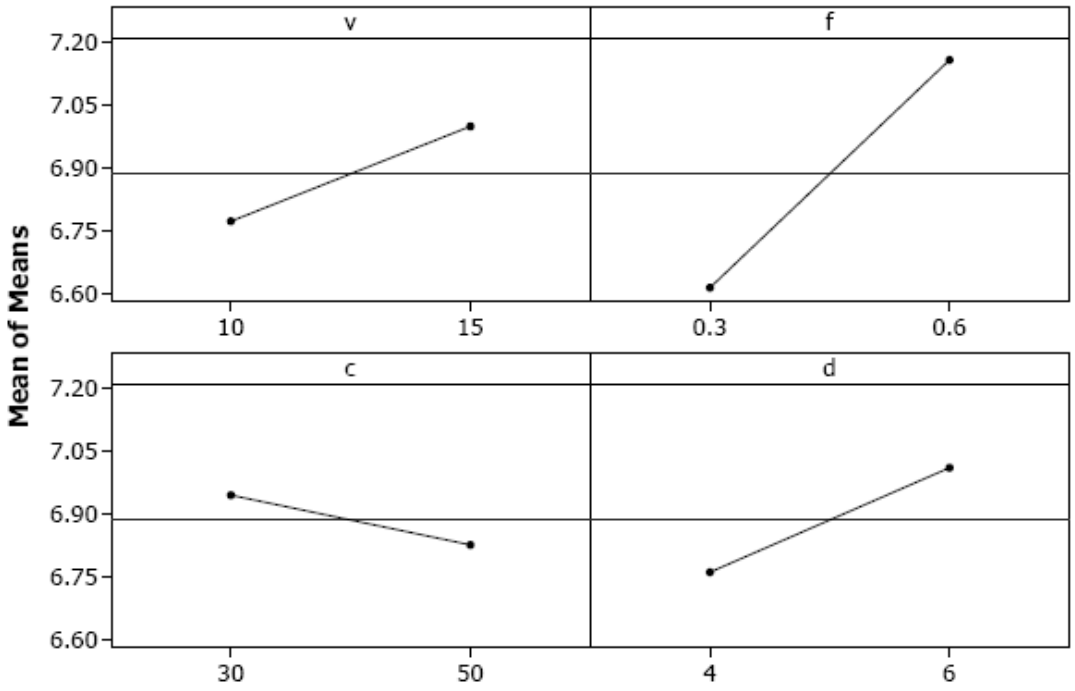

Figure 5.5: Main effect Plot for OC-depth

In Table 5.9, ANOVA of OC-depth is presented with all the terms. The significant factors are Voltage, Feed, electrolyte concentration and diameter of tube, whereas all interactions factors are found to be insignificant. After eliminating non-significant sources i.e. interaction of process parameter like V*F, V*D, V*D, F*C, F*D, C*D terms, the results are shown in Table 5.10.

Table 5.9: ANOVA for OC-depth

Source	DF	Seq. SS	Adj. SS	Adj. MS	F	P
Volt (V)	1	0.20430	0.20430	0.20430	548.91	0.000
Feed (F)	1	1.17723	1.17723	1.17723	3162.88	0.000
Electrolyte Concentration(C)	1	0.05617	0.05617	0.05617	150.91	0.000
Diameter (D)	1	0.24751	0.24751	0.24751	664.98	0.000
V*F	1	0.01277	0.01277	0.01277	34.31	0.002
V*C	1	0.00303	0.00303	0.00303	8.13	0.036
V*D	1	0.00001	0.00001	0.00001	0.03	0.863
F*C	1	0.00078	0.00078	0.00078	2.11	0.206
F*D	1	0.00748	0.00748	0.00748	20.10	0.006
C*D	1	0.00714	0.00714	0.00714	19.18	0.007
Error	5	0.00186	0.00186	0.00037		
Total	15	1.71828				

Table 5.10: ANOVA for OC-depth after eliminating non-significant values

Source	DF	Seq. SS	Adj. SS	Adj. MS	F	P
Volt (V)	1	0.20430	0.20430	0.20430	67.95	0.000
Feed (F)	1	1.17723	1.17723	1.17723	391.53	0.000
Electrolyte Concentration(C)	1	0.05617	0.05617	0.05617	18.68	0.001
Diameter (D)	1	0.24751	0.24751	0.24751	82.32	0.000
Error	11	0.03307	0.03307	0.00301		
Total	15	1.71828				

In Table 5.11 the main effects of voltage, feed, electrolyte concentration and diameter of electrode are 0.226, 0.543, 0.119 and 0.249, respectively, on overcut-depth in mm, in order of significance. In which there feed rate is important factor and then tool diameter then voltage and lastly electrolyte concentration.

Table 5.11: Taguchi analysis response table for OC-depth

Level	Voltage (V)	Feed (F)	Concentration (g/l)	Diameter (mm)
1	6.775	6.616	6.947	6.763
2	7.001	7.159	6.828	7.012
Delta	0.226	0.543	0.119	0.249
Rank	3	1	4	2

Table 5.12: Estimated Model Coefficients for Means of OC-depth

Term	Co-eff.	SE Co-eff.	T	P
Constant	6.88750	0.01371	502.431	0.000
V 10	-0.11300	0.01371	-8.243	0.000
F 0.3	-0.27125	0.01371	-19.787	0.000
C 30	0.05925	0.01371	4.322	0.001
D 4	-0.12438	0.01371	-9.073	0.000
S = 0.05483	R-Sq. = 98.1%		R-Sq.(adj.) = 97.4%	

The coefficients of model mean of means for over cut depth is shown in Table 5.12 and parameter result are standard deviation of error S=0.05483, amount of variation R^2 = 98.1% and R^2 (adj.) = 97.4%. And comparing the P value is less than or equal to 0.05 it can be concluded that the effect is significant, otherwise not significant.

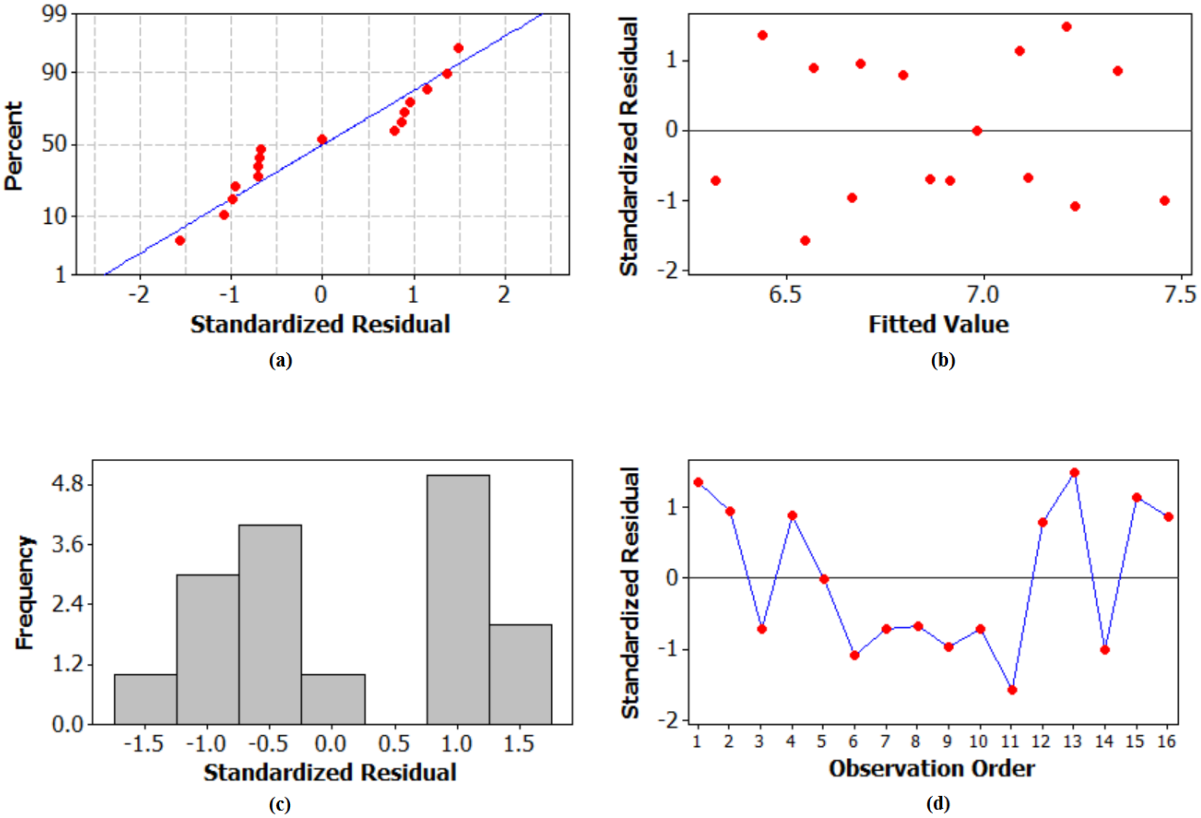

Figure 5.6: Residual Plots for OC-depth. (a) Normal probability plot (b) Residual vs. Fitted plot (c) Histogram of Residuals (d) Residuals vs. Order of data plot

The residual plot for over cut is shown in Figure 5.6. This residual plot in the graph for normal probability plot indicates the data are normally distributed and variables are influencing the response. And the Residuals versus fitted value indicate the variation is constant. And the Histogram proved the data are not normally distributed it may be due to the

fact that the number of points are very less. And Residual versus order of the data indicates that there are systematic effects in the data due to data collection order.

5.2. Conclusion:

The work evaluates the feasibility of machining blind cavity on AISI P20 tool steel in ECM with Rotary U-shaped electrode. Among the four process parameters, feed rate influences highly the responses followed by voltage and then electrode diameter. Electrolyte concentration has very little effect on Response.

Chapter 6

Conclusion

In the present study, four factors are considered voltage, feed rate, electrolyte concentration and tool diameter. AISI P20 steel as a work-piece and 16 experiments to be conducted to obtain an optimum level in achieving high material removal rate, minimize OC-diameter and minimize OC-depth. The following conclusions are arrived:

- Among the four process parameters, feed rate influences highly the MRR, followed by applied voltage then electrode diameter and then by the concentration of electrolyte.
- For both OC-diameter and OC-depth the most influencing parameter are feed rate followed by electrode diameter then voltage and lastly the concentration of electrolyte.
- From the grey relation grade, the optimal machining parameter setting are obtained for Run 15 i.e. voltage = 15 V, feed = 0.6 mm/min, electrolyte concentration = 50 g/l and electrode diameter = 4 mm for maximizing MRR and minimizing overcut diameter and depth.

References

[1] J.A. McGeough, *Principle of Electrochemical Machining*, Chapman and Hall, London, 1974.

[2] H. El-hofy, *Fundamentals of Machining Processes*, Conventional and Nonconventional Processes, Taylor & Francis Group, 2007.

[3] D. Zhu, K. Wang, J.M. Yang, *Design of Electrode Profile in Electrochemical Manufacturing Process*, CIRP Annals-Manufacturing Technology 52 (1) 169-172.

[4] YUMING ZHOU and JEFFREY J. DERBY, *The Cathode Design Problem in Electrochemical Machining*, Chemical Engineering Science, 50(17) (1995) 2679- 2689.

[5] C.S. CHANG, L.W. HOURNG, C.T. CHUNG, *Tool design in electrochemical machining considering the effect of thermal-fluid properties*, Journal of Applied Electrochemistry, 29 (1999) 321-330.

[6] S.J. Ebeid, M.S. Hewidy, T.A. El-Taweel, A.H. Youssef, *Towards higher accuracy for ECM hybridized with low-frequency vibrations using the response surface methodology,* Journal of Materials Processing Technology 149 (2004) 432-438.

[7] P.S.Pa, *Effective form design of electrode in electrochemical smoothing of end turning surface finishing*, Journal of materials processing technology 195 (2008) 44-52.

[8] Chunhua Sun, Di Zhu, Zhiyong Li, Lei Wang, *Application of FEM to tool design for electrochemical machining freeform surface,* Finite Elements in Analysis and Design 43 (2006) 168-172.

[9] J.A. Westley, J. Atkinson, A. Duffield, *Generic aspects of tool design for electrochemical machining,* Journal of Materials Processing Technology 149 (2004) 384-392.

[10] M.S. Amalnik, J.A. McGeough, *Intelligent Concurrent Manufacturability Evaluation of Design for Electrochemical Machining,* Journal of Materials Processing Technology 61 (1996) 130-139.

[11] K.P. Rajurkar and M.S. Hewidy, *Effect of Grain Size on ECM Performance,* Journal of Mechanical Working Technology, 17 (1988) 315 - 324.

[12] K.P. Rajurkar, D. Zhu, B. Wei, *Minimization of Machining Allowance in Electrochemical Machining,* Annals of the CIRP Vol. 47(1998) 165-168.

[13] M.S. Hewidy, *Controlling of metal removal thickness in ECM process,* Journal of Materials Processing Technology 160 (2005) 348-353.

[14] I. Strode and M. B. Bassett, *The effect of Electrochemical Machining on the Surface Integrity and Mechanical Properties of Cast AND Wrought Steels,* Wear, 109 (1966) 171- 180.

[15] Ming-Chang Jeng, Ji-Liang Doong and Chih-Wen Yang, *The effects of carbon content and microstructure on the metal removal rate in Electrochemical Machining,* Journal of Materials Processing Technology, 38 (1993) 527-538.

[16] S.C. TAM, N.H. LOH, *Optimization of the ECM-Abrasive Polishing of Mild Steel Using Response Surface Methodology,* Journal of Mechanical Working Technology, 19 (1989) 109-117.

[17] J.J. Sun, E.J. Taylor, R. Srinivasan, *MREF-ECM process for hard passive materials surface finishing,* Journal of Materials Processing Technology 108 (2001) 356-368.

[18] Shuo-Jen Lee, Yu-Ming Lee, Ming-Feng Du, *The polishing mechanism of electrochemical mechanical polishing technology,* Journal of Materials Processing Technology 140 (2003) 280–286.

[19] H. Hocheng, P.S. Pa, *The application of a turning tool as the electrode in electropolishing,* Journal of Materials Processing Technology 120 (2002) 6-12.

[20] Baocheng Wang and Jinhua Zhu, *Effect of electrochemical polishing time on surface topography of mild steel,* Journal of University of Science and Technology 14 (2007) 236-239.

[21] A.K.M. De Silva **,** H.S.J. Altena**,** JA. McGeough, *Influence of Electrolyte Concentration on Copying Accuracy of Precision-ECM,* Annals of the CIRP, 49.

[22] Petr Novak, Ivo Rousar, Rudolf Stefec, Vladmir Cihal, *Intergranular corrosion in Electrochemical Machining,* Materials Chemistry and Physics 10 (1984) 155-161.

[23] M.A. Bejar and F. Gutierrez, *On the determination of current efficiency in electrochemical machining with a variable gap,* Journal of Materials Processing Technology, 37 (1993) 691-699.

[24] M.A. Bejar, F. Eterovich**,** *Wire-electrochemical cutting with a NaNO3 electrolyte,* Journal of Materials Processing Technology 55 (1995) 417- 420.

[25] T. Haisch, E. Mittemeijer, J.W. Schultze, *Electrochemical machining of the steel 100Cr6 in aqueous NaCl and $NaNO_3$ solutions: microstructure of surface films formed by carbides,* Electrochimica Acta 47 (2001) 235–241.

[26] D. Zhu, W. Wang, X.L. Fang, N.S. Qu, Z.Y. Xu, *Electrochemical drilling of multiple holes with electrolyte-extraction*, CIRP Annals - Manufacturing Technology 59 (2010) 239–242.

[27] Xiangyu Zhao, Liqun Ma, Meng Yang, Yi Ding, Xiaodong Shen, *Electrochemical properties of Ti–Ni–H powders prepared by milling titanium hydride and nickel*, international journal of hydrogen energy xxx (2009) 1-4.

[28] Minghuan Wang,Wei Peng ,Chunyan Yao, *Electrochemical machining of the spiral internal turbulator*, International Journal of Advanced Manufacturing Technology 49 (2010) 969–973.

Dissemination of Work

Published

1. Rahul Ganjir, C.K.Biswas and Shailesh Dewangan,, "Estimation of MRR on Electrochemical Machining by using Taguchi Method", *International Conference on Innovative Science & Engineering Technology, (ICISET-2011),* pp 362-365, 8-9 April, 2011, Rajkot, India.